NORLEUAL, AN ANGIOTENSIN IV RECEPTOR LIGAND AND C-MET ANTAGONIST

By

BRENT JOSEPH YAMAMOTO

A dissertation submitted in partial fulfillment of
The requirements for the degree of

DOCTOR OF PHILOSOPHY

WASHINGTON STATE UNIVERSITY
Program in Pharmacology and Toxicology

AUGUST 2006

To the Faculty of Washington State University:

The members of the Committee appointed to examine the dissertation of BRENT JOSEPH YAMAMOTO find it satisfactory and recommend that it be accepted.

_____
Chair

_____

_____

_____

ACKNOWLEDGMENT

I would like to thank my inspiring mentor and noble friend, Dr. Joe Harding for wisdom, guidance, and support throughout my experience at Washington State University. I would not be where I am today if Dr. Harding had not given me a chance to volunteer in his lab.

I would also like to thank the members of the Harding Lab, past and present, for support and cooperation on all my research experiments. I would like to thank Alex Masino for instruction and assistance during the early phases of the project. Additionally I would also like to thank Patrick Elias for contributions of the scattering assays and continuous support and advice. I am also thankful to Christina Russert and Bryan Hudson and the entire Harding and Wright labs for technical assistance with the toxicological studies and lab support. I would also like to thank the members of my committee, Dr. Howard Hoscik, Dr. Michael Varnum, and Dr. John Wright. Their insights and advice have been innovative and invaluable. Lastly, I would like to thank my Mother, Father, Sister and Brother, and Carrie, for unconditional love and support through all my endeavors.

NORLEUAL, AN ANGIOTENSIN IV RECEPTOR LIGAND

AND C-MET ANTAGONIST

ABSTRACT

By Brent Joseph Yamamoto, Ph.D.
Washington State University
August 2006

Chair: Joseph W. Harding

In 2005, 1.4 million new cases of cancer were diagnosed, resulting in over half a million deaths. Despite improved diagnostic procedures, the mortality rate from cancer has changed little over the last two decades. This lack of progress can be directly linked to the continued reliance on surgery, cytotoxic chemotherapeutic agents, and radiation therapy as the primary treatment methods coupled with the lack of new therapeutic approaches. For this reason, novel and effective therapies must be developed to combat aggressive forms cancer. The use of angiotensin IV (AT_4) receptor antagonists represents such a therapy.

The previous efforts of Masino, Hosick, Wright, and Harding demonstrated that Norleual exhibits anti-cancer efficacy on murine mammary primary tumor growth, metastasis, and angiogenesis in vivo. However, the mechanism of action, side effects, and potential usefulness of Norleual in other cancer variations remained unknown. In this dissertation, we demonstrate that the AT_4 ligand, Norleual, antagonizes the hepatocyte growth factor/c-Met receptor

tyrosine kinase system. In addition, we show that Norleual exhibits anti-cancer activity in epithelial derived cancers such as murine mammary and melanoma. Furthermore, we observe that healthy mice treated chronically with Norleual exhibit a phenotype with significantly reduced percent body fat. Lastly, a blinded general pathological assessment revealed that Norleual was relatively non-toxic. The only significant finding, however, was that Norleual treated animals presented significantly fewer lipid vacuoles in the liver. Remarkably, the treated mice were similar to control mice in every other gross and microscopic pathological aspect assessed.

These findings suggest that the AT_4 antagonist, Norleual exerts its effects by antagonizing the HGF/c-Met system. This discovery is significant because c-Met is involved in a variety of biological processes ranging from development to carcinogenesis. Moreover, we observe that AT_4 antagonists are not only efficacious in mouse cancer models, but are also relatively non-toxic. In conclusion, these findings provide new insight into the workings of the AT_4 receptor and identify a new family of c-Met antagonists that may allow novel cancer treatment strategies, lower the cost of therapy and thus improve accessibility regardless of socioeconomic status.

TABLE OF CONTENTS

Page

ACKNOWLEDGMENT iii

ABSTRACT iv

LIST OF TABLES viii

INTRODUCTION 1

Understanding cancer 1

Why cancer is lethal 3

Integral role of angiogenesis in cancer 4

Angiogenesis is a target for cancer therapeutics 6

The angiotensin pathway 7

AT_4 antagonists, potential caner therapeutics 7

Materials and methods 11

References 17

MANUSCRIPT I, NORLEUAL, AN AT_4 RECEPTOR LIGAND, IS A C-MET ANTAGONIST AND REPRESENTS A NEW CLASS OF ANTI-CANCER DRUGS 19

Introduction 19

Text 20

Acknowledgments 41

MANUSCRIPT 2, NORLEUAL INHIBITS MURINE MELANOMA IN VIVO 44

Abstract 44

Introduction 44

Materials and Methods 46

Results 48
Discussion 50
References 55
MANUSCRIPT 3, TOXICOLOGICAL STUDY OF NORLEUAL IN A C-57BL/6 MURINE MODEL 56
Abstract 56
Introduction 56
Materials and Methods 57
Results 60
CONCLUSION 71

LIST OF TABLES

1. Densitometry of HUVEC-ECM arrays……..…14

2. Densitometry of murine mammary tumor angiogenesis arrays…..…...…16

LIST OF FIGURES

1. Norleual and Nle[1]AngIV modulate ECM related genes in HUVECs……..13
2. Norleual modulates angiogenic genes in murine mammary tumors……..15
3. Norleual and HGF compete for binding with ^{125}I-Norleual and ^{125}I-HGF….32
4. Norleual inhibits HGF dependent Met phosphorylation and Gab1 association and phosphorylation in vitro 1……..34
5. Norleual inhibits HGF induced cell scattering in MDCK cells……..36
6. Norleual inhibits angiogenesis and melanoma growth……...37
7. Norleual inhibits HGF dependent Met phosphorylation and Gab1 association and phosphorylation in vitro 2……39
8. *In vivo* inhibition of murine melanoma cancer growth by Norleual via systemic delivery…..……52
9. *In Vivo* inhibition of murine melanoma cancer growth by Norleual via in situ delivery……53
10. Norleual exhibits non-classical dose response in murine melanoma cancer via systemic delivery……54
11. Growth profiles for control and Norleual treated mice……..65
12. DXA analysis of Norleual treated and Control mice……66
13. Pathological assessment……..68

INTRODUCTION

Understanding cancer

Cancer is a disease resulting from an accumulation of genetic mutations. These changes cause altered function in proto-oncogenes leading to dysregulation of DNA repair, proliferation, and apoptotic signaling (Hill, 1998). Normally, compensatory pathways enable the cell to retain normal control even after one or two oncogenes have been mutated. However, additional mutations may render these built-in compensatory mechanisms inoperable. When sufficient oncogenes are activated, the end result is a transformed or 'run-away' cell that no longer conforms to the normal constraints of cell cycle and cell death processes (Evan, 2001). These oncogenes include, but are not limited to, growth factors, receptor and non-receptor tyrosine kinases, G-proteins and G-protein receptors, serine/threonine kinases, nuclear transcription factors, and regulators of apoptosis.

Oncogenic activation is the result of modifications to the DNA. Causes vary from a wide range of phenomena. Mutations in DNA or malfunctions in DNA replication, viruses (insertional mutagenesis), chromosomal translocation, or any other event leading to an error in the DNA sequence, has the potential to modify a critical location of the genome. In the cell cycle, this oncogenic activation may trigger signaling events that circumvent cell cycle checkpoints (cyclin and cyclin-dependent-kinases (CDKs)), and mitosis cannot be disengaged (Alberghina, 2001). An example of this is the control of the G_1 to S phase transition by cyclin

D1. Cyclin D1 activates CDKs 4 and 6 that subsequently phosphorylate retinoblastoma (Rb). This phosphorylation of Rb relseases the E2F transcription factor that activates S-phase required genes. Alternatively, if the signaling mechanisms in apoptosis are compromised by oncogenes activation, the cell cannot appropriately respond to self-destruct signals that are normally initiated upon injury, age, or un-repairable DNA damage (Hill, 1998).

In one sense, cancer can be thought of as a probability event. Spontaneous mutations are occurring to our DNA quite frequently at a frequency of 10^{-7} per cell per generation (Hill 1998). However, the alteration must be in a critical location to activate an oncogene. Our genome contains buffering zones of filler DNA, called introns. Introns provide spacing between expressed DNA, exons (however proto-oncogenes may reside throughout the genome, in exons and introns). Furthermore, evolution has provided the ability to repair any errors in the DNA code via proofreading. Nevertheless, proofreading is not a flawless system and some DNA errors are able to evade this safeguard mechanism. Thus any mutation, whatever the cause, has the probability of activating an oncogene. Factors that contribute to mutagenesis include genetic predisposition, diet, exposure to carcinogens (smoking), chronic inflammation, reproductive status, epigenetics, age, and of course, chance (Michor, 2004).

In addition to these repair pathways, the immune system plays a protective role in cancer. It has been reported that tumor cells display differential, “non-self” antigens that the immune system can recognize and mount

an immune response to. However, further mutations may enable the tumor cell to circumvent detection and eradication by the immune system.

Once a cell has activated enough oncogenes, it will no longer respond to the regulatory signals initiated by governing pathways. The transformed cell now clonally evolves into heterogeneous population through further mutations and selection. The malignancy cannot be stopped by any endogenous means and continues to grow uncontrollably. The cancer has begun.

Why cancer is lethal

Cancer mortality is caused by organ failure due to metastatic growth. Metastases are distant satellite growths arising from the primary tumor. An established malignant primary tumor will slough off approximately 10^7 - 10^9 cells/day into the circulatory/lymphatic systems. However, less than 0.01% of the circulating cancer cells succeed in developing into a distant site neoplasia (Fidler, 2003). This finding raises the question as to whether or not metastasis is a haphazard or a designed occurrence. Although the answer is not entirely clear, it is evident that one, the tumor cells must travel to the distant site, and two, the site must present a microenvironment that is suitable for the cancer cell to proliferate. This is activity is called the metastatic process.

The metastatic process can be outlined in five steps. First, cells detach from the primary tumor followed by vascular or lymphatic invasion; second, cells are transported and survive in the circulation; third, the cells arrest at a new location; fourth, the cells extravasate from the vasculature into the parenchyma;

and fifth, the cells proliferate. In time, many neoplasms will accumulate and grow uncontrollably. Soon, growths located in non-vital areas become so massive that they interfere with normal tissue and organ functions. In addition, metastases deplete the body's resources and overwhelm the nutrient delivery/waste removal capabilities of the body. This 'parasitic' nature of cancer is evident in the 'wasting away' of patients in latter stages of terminal cancers. Unfortunately, metastatic growths often spread to vital organs and lead to the loss of function (i.e. lungs) and results in death.

Integral role of angiogenesis in cancer

As unrelenting and unstoppable as cancer growth may seem, it is dependent upon sustenance from the host. As tumor size increases, so does the requirement for nourishment. It has been recognized that pre-existing blood supply found in normal tissues cannot sustain large tumor masses. Accordingly, cancer has developed a way to circumvent this obstacle by recruiting its own blood supply. As a tumor cell replicates exponentially, the tumor grows (to approximately 1-2 mm^3) to a point where the existing blood supply (limited by preexisting vasculature) can no longer support any additional growth (Folkman, 1971). It is at this growth/blood supply threshold where hypoxic cancer cells stimulate additional blood vessel growth, angiogenesis. Under normoxic, or oxygen rich conditions, hypoxic inducible factor 1-α (HIF-1) is hydroxylated on its oxygen dependent degradation domain (ODDD) in an oxygen dependent manner. This hydroxylation is recognized by Von Hippel-Lindau tumor

suppressor protein (pVHL) and HIF-1α is subsequently ubiquitinated and degraded by proteolysis. This process is further regulated by acetylation by an N-acetyl-transferase, ARD1 that accelerates the degradation process. The literature also reports activation of HIF-1α by ERK p44/42 phosphorylation. However, it is not entirely clear that this regulation is involved in hypoxic signaling. Under hypoxic conditions, HIF-1α is not hydroxylated and is thus stabilized. HIF-1α heterodimerizes with HIF-1β forming activated HIF-1 and translocates to the nucleus. Activated HIF-1 drives the transcription of at least 60 gene products that include glucose transporters, glycolytic enzymes, endothelien-1, angoipoetin-2, platelet derived growth factor-B, and c-Met (Scarpino, 2004, Pennacchietti, 2003).

Today it is known that Met is a critical player that contributes to carcinogenesis, tumor development and growth, and tumor angiogenesis. Scientists now know that dysregulation of Met signaling is an unusually common, yet significant feature of many human malignancies (Christensen, 2005). This characteristic is due to the ubiquitous conservation of Met expression in cells of epithelial and endothelial origin. In cancer, tumor cells often over-express HGF and/or Met. This malfunction contributes to enable tumor cells to proliferate, migrate, invade, and escape apoptosis. Furthermore, tumor secreted HGF contributes to tumor angiogenesis by activating HGF receptors located on vascular endothelial cells. Tumor angiogenesis begins with stimulated endothelial cells activating proteases that degrade the nearby extracellular matrix (ECM). This enables the endothelial cell to breach the basement membrane and

relocate in the stroma. Once this is achieved, the endothelial cells proliferate and ultimately form tubular structures with other cell types that can fuse with other blood vessels to form a vascular network. However, this process is not as finely orchestrated as in embryogenesis, corpus luteum formation, wound healing, or adipose tissue development. These newly formed blood vessels are poorly constructed and chaotic in nature. As a consequence, these blood vessels are leaky and provide sporadic blood flow or are even non-functional (Carmeliet and Jain, 2000). Thus, hypoxic regions where the blood supply will be non-uniform and result in poor delivery of oxygen and nutrients and inadequate clearance of metabolic waste will remain. Furthermore, the mechanical forces from the tumor mass compress blood vessels to further reduce blood delivery. These customary phenomenons of tumor angiogenesis pose complications of lower bioavailibility of systemically delivered cancer drugs and hypoxic resistance to radiation and/or chemotherapeutic agents. Despite these shortfalls, the tumor vasculature provides blood flow to sustain the growing tumor mass, enabling the tumor to expand.

Angiogenesis is a target for cancer therapeutics

In 1972, Judah Folkman first exposed the idea that limiting the blood supply to tumors by inhibiting the growth of blood vessels (anti-angiogenesis) into tumors might represent a viable anti-cancer treatment strategy. This epiphany subsequently spawned an entire new field of cancer therapeutics that resulted in impressive advancements in our basic understanding of the angiogenic process.

The recently FDA approved anti-angiogenic drug Avastin marks the milestone in this type of drug development (USDA, 2003).

The angiotensin pathway

The 'classic' renin angiotensin system has been well classified to regulate blood pressure. As a result, this pathway became a successful drug target, chiefly angiotensin converting enzyme (ACE) antagonists that prevent the enzymatic conversion of angiotensin I to angiotensin II. This prevents subsequent activation of the angiotensin II (AT_1) receptor, leading to a reduction in blood volume. Previously, it had been assumed that smaller fragments of the angiotensinogen sequence shorter than angiotensin II were biologically inert. However, it was later discovered that the degradation product of angiotensin II (Asp-Arg-Val-Tyr-Ile-His-Pro-Phe), angiotensin IV (Val-Tyr-Ile-His-Pro-Phe), has biological activity. Further studies confirmed that these angiotensin IV induced physiological perturbations were independent of the AT_1 or AT_2 receptors and directed through a new receptor called the angiotensin IV (AT_4) receptor (Harding, 1992). Since this discovery, the AT_4 receptor system has been shown to play an integral role in regulation of blood flow, behavior, and cognitive function (Wright and Harding, 2004, Kramar 1997, Davis, 2006).

AT_4 antagonists, potential caner therapeutics

Initial interest in a possible relationship between the AT_4 receptors and cancer was based on a combination of experimental findings generated in our

laboratory and novel concepts (at the time) regarding the importance of angiogenesis to tumor growth and metastasis.

Our laboratory has shown that AT_4 receptor antagonists, chiefly our lead compound, Norleual, inhibits endothelial cell growth in vitro, blocks angiogenesis ex vivo, inhibits primary tumor growth, metastasis, and neovascularization in a mouse mammary cancer model with in situ and systemic delivery (Masino and Harding, unpublished). Additionally, we observed that Norleual deactivates a plethora of ECM and pro-angiogenic related genes in human umbilical vein endothelial cells (HUVEC) (Figure 1 and Table 1) and in mouse mammary tumors (Figure 2 and Table 2). These observations demonstrate the biological potency of AT_4 ligands. However, at this time, the mechanism of action of Norleual remained an enigma.

. Earlier studies have suggested that the biological activity of AT_4 ligands was attributable to interactions with a protease, insulin regulated aminopeptidase (IRAP) (Albiston, 2001). It was believed that the physiological action of AT_4 ligands resulted from their ability to competitively inhibit IRAP's enzymatic activity causing a gradual accumulation of yet-to-be identified endogenous peptide substrates. Despite this seemingly attractive hypothesis, many aspects of the IRAP inhibition hypothesis do not emulate the established characteristics of AT_4 receptor signaling. First, the AT_4 system can be activated or inhibited by agonists or antagonists. This phenomenon is difficult to reconcile based on enzyme/substrate interactions. Second, the time frame for peptidase inhibitors to alter endogenous levels of bioactive peptides is many minutes to hours. By

contrast, the observed signal transduction and physiological changes attributed to the AT_4 receptor system occur in seconds (Wright and Harding, 2004). Third, although the established biological activity of AT_4 ligands is subnanomolar to subpicomolar (8, 9), the reported Ki of the AT_4 receptor ligand, Nle^1AngIV (Nle-VIHPF), for IRAP is >0.3 micromolar (Lew, 2003). Therefore, these fundamental discrepancies between IRAP and AT_4 obligated us to believe that IRAP was a red herring. Because the number of IRAP proteins on the cell surface is very large when compared to numbers of c-Met receptors (Hanesworth, 1993) and Higuchi, 1991), binding of AT_4 ligands to c-Met was all but invisible.

Consequently, the conclusions drawn from prior AT_4 studies were fundamentally flawed and the true mechanism of biological activity was masked. This suggested that another identified protein or proteins was responsible for the action of AT_4 receptor ligands. Therefore, it was the goal of this dissertation to shed light on the true mechanism of AT_4 ligands. In chapter two, we present evidence and discuss the apparent mechanism of action of Norleual as a c-Met antagonist in molecular, in vitro, ex vivo, and in vivo assays. In chapter three, we demonstrate the potential applicability of Norleual as a cancer therapy by showing anti-tumor activity in a murine melanoma model. Additionally, we show that Norleual can be delivered through various delivery methods and sites while retaining anti-cancer efficacy. In chapter four, we present findings from a preliminary toxicological study. We observed that chronic administration of Norleual to healthy C57 mice resulted in significant weight loss attributed to reduced fat deposition and not lean body mass. Furthermore, we observe no

major organ complications from a blinded pathological assessment. The only remarkable feature observed in the pathology study was fewer hepatic lipid vacuoles in the Norleual treated animals. These findings are consistent with predicted c-Met antagonist behavior. Together these findings suggest that Norleual is a potent inhibitor of the c-Met system and the observed toxicity is relatively low.

Finally, this dissertation concludes by commenting on questions about the future of AT_4 receptor research and beyond.

Materials and methods

Cell culture

HUVECS were grown in EGM-2 (endothelial growth media-2) (Cambrex). Cells were grown in 100mm plates to 95% confluentcy and split 1:6. Drug treatements were administeried in EGM-2 and media and drug was replaced every 48 hours. On day eight, RNA was harvested and RNA expression was analyzed on mouse ECM arrays (HS-010, SuperArray).

Murine mammary cancer model

Mice were anesthietized and ~500,000+SA cells (in 100ul) were injected into bilateral mammary glands. Simutaneously, a pre-primed osmotic pump (Alzet micro-osmotic pump model 1002) was implanted intra peritonealy (skewed along the ventral midline). Sutures and wound clips were used to close and the mice were monitored during recovery. The mice were checked daily for healing progression and primary tumor development (by palpation). Palpated tumors were measured with digital calipers. On day 14, new pumps were implanted. On day 25 the mice were sacrificed and the tumors were removed and weighed. Immediately after weighing, the tumors were flash frozen in liquid nitrogen and stored at –70°C. The next day, RNA was harvested and RNA expression was analyzed on mouse angiogenesis arrays (MM-009. SuperArray)

Gene Arrays

Total RNA was harvested using the GenElute RNA purification system (Sigma) per manufacturer's protocol. Biotin-dUTP was incorporated into cDNA

probes were reverse-transcribed from the extracted RNA (SuperArray AmpoLabeling-LPR kit).

The labeled probes were then hybridized to the microarrays and the image was visualized on x-ray film. The image was digitized and analyzed using TotalLab. The intensities were normalized to glyceraldehyde phosphate dehydrogenase and Norleual and Nle[1] AngIV signals were compared to normalized control values. Differences were expressed as fold increases or decreases. Arrays were perfomred in duplicate for the HUVECS and in triplicate for the primary mammary tumors. Arrays, reagents, and other required kits were purchased from SuperArray. Biotin-16-dUTP was purchased from Enzo biochemicals.

FIGURE 1

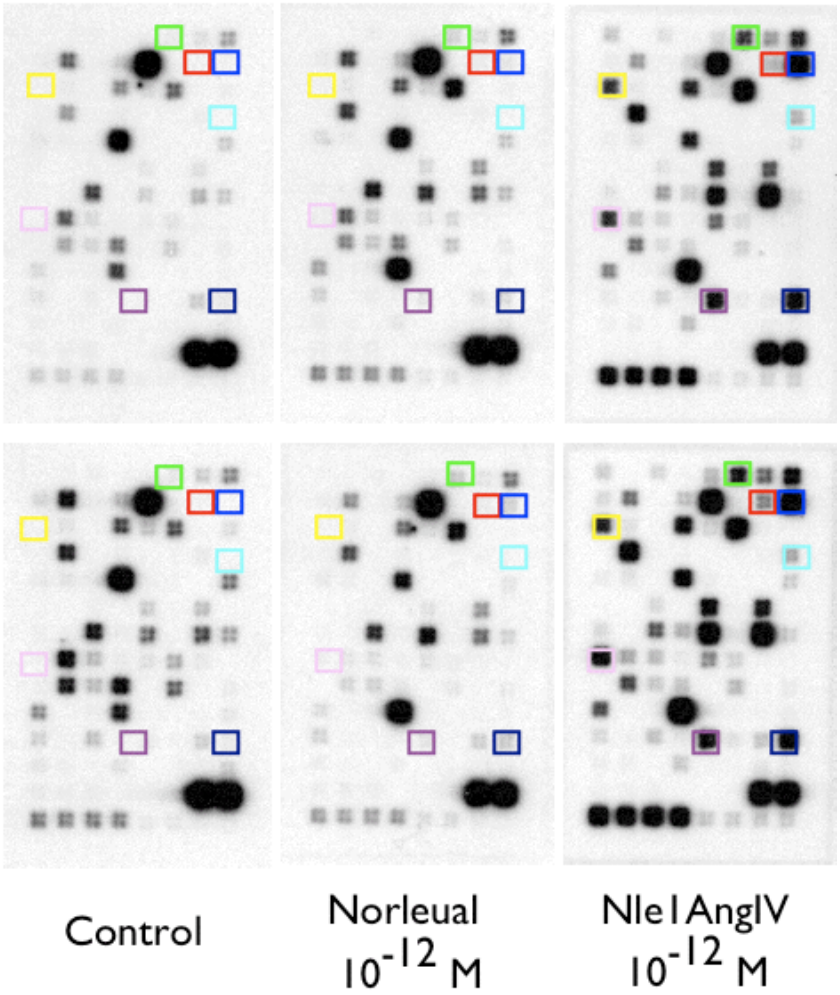

Figure 1. Norleual and Nle^{1}AngIV modulate ECM related genes in HUVEC. HUVECS were treated for eight days in the presence or absence of Norleual or Nle^{1} AngIV at a concentration of 1 pM. RNA was harvested and transcriptional activity of 96 ECM related genes were assessed using SuperArray gene microarrays. Arrays were performed in duplicate. Densitometry analysis was performed. Genes that differed from control at least two-fold are hi-lighted by a colored box.

TABLE 1

Gene	GenBank	HUVEC Norleual 10^{-12} M Fold Change* from Control (n=2)	HUVEC Nle[1] Ang IV 10^{-12} M Fold Change* from Control (n=2)	
ADAMTS 1	NM_006988	None	+6.08	
Caspase 8	NM_001228	None	+3.81	
Caveolin 1	NM_001753	None	+2.11	
CD44	NM_000610	+3.15	+14.37	**Green
Cadherin 1	NM_004360	None	+5.18	
CECAM 5	NM_004363	None	+3.50	
Catenin α–like–1	NM_003798	+2.61	+19.46	**Red
Catenin β	NM_001904	+4.67	+54.79	**Blue
Catenin δ1	NM_001331	None	+15.60	**Yellow
Cathepsin L	NM_001912	None	+2.73	
Fibronectin 1	NM_002026	None	+2.22	
Integrin α2	NM_002203	+2.44	+24.20	**Light Blue
Integrin β1	NM_002211	None	+8.11	
Integrin β3	NM_000212	+2.54	+6.23	
Integrin β8	NM_002214	None	+5.66	
Laminin β1	NM_002291	+2.79	+4.77	
Hyaluronidase	NM_012215	None	+4.06	
MMP 1	NM_002421	None	+14.93	**Pink
MMP 10	NM_002425	Inconclusive	-2.14	
MMP 13	NM_002427	None	+7.84	
MMP 24	NM_006690	None	-2.05	
MMP 9	NM_004994	None	+2.41	
PECAM 1	NM_000442	+2.20	+2.47	
PAI-1	NM_000602	+2.61	+28.90	**Purple
Thrombospondin 1	NM_003246	+2.55	+19.48	**Navy Blue
TIMP 2	NM_003255	None	+4.00	
Cyclophilin A	NM_021130	None	+4.73	
PUC18	L08752	None	None	
GAPDH	NM_002046	None	None	

Table 1 Densitometry of HUVEC ECM arrays. Only genes that showed a two-fold or greater difference from control are presented (*). The color corresponds to the location of the genes in figure 1 with 10-fold or greater changes when compared to control (**).

FIGURE 2

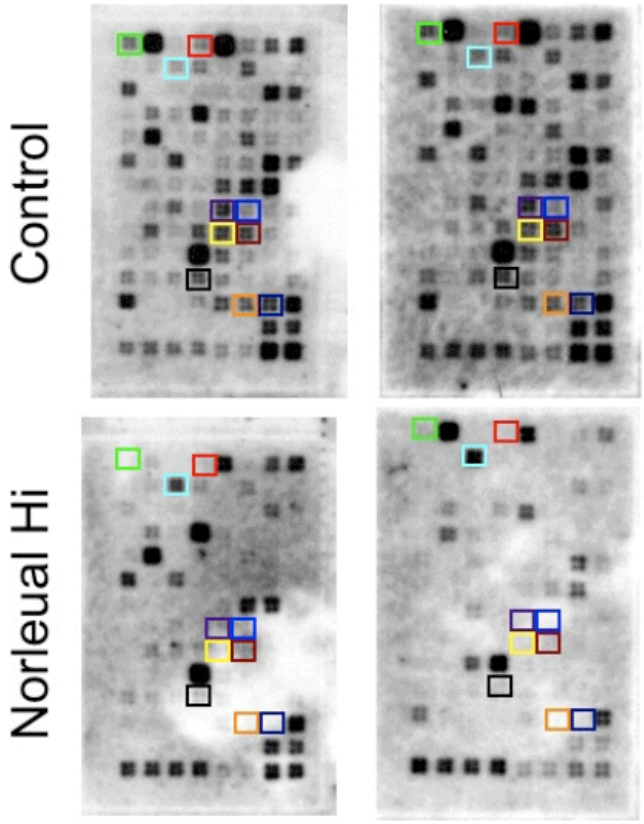

Figure 2. Norleual modulates angiogenic genes in murine mammary tumors. Balb/c mice grafted with +SA murine mammary cancer cells were treated with Norleual. After 28 days of IP drug administration via an osmotic pump (1mg/kg/day). Primary tumors were harvested and RNA was harvested. Trascriptional activity of 96 angiogenisis related genes were assessed using SuperArray gene microarrays. Arrays were performed in duplicate. Densitometry analysis was performed. Genes that differed from control at least five-fold are hi-lighted by a colored box.

TABLE 2

Gene	GenBank	Breast Cancer Primary Tumor Norleual Hi treatment Fold Change from Control (n=2)	
Adamts 1	NM_009621	-11.2	*Green
Angiopoietin 1	NM_009640	-3.7**	
Angiopoietin 2	NM_007426	-4.5	
CD 36	NM_007643	-77.3	*Red
Connective tissue growth factor	NM_010217	+5.3	*Light Blue
Ephrin A5	NM_007909	-2.5	
EGF-R	NM_007912	-4.6	
Coagulation Fact 2	NM_010168	-2.0	
FGF 16	NM_030614	-4.3	
FGF-R 3	NM_008010	-6.2	
Hif 1a	NM_010431	-3.8	
Il-10	NM_010548	-4.8**	
IL-12a	NM_008351	-3.0**	
Integrin a5	NM_010577	-2.3	
Integrin aV	NM_008402	-4.0	
MMP 9	NM_013599	-3.5	
PDGF b	NM_011057	-4.2	
PDGF-R a	NM_011058	-2.0	
Pecam 1	NM_008816	-11.1	*Purple
Cxcl 4	NM_019932	-29.2	*Blue
Plasminogen activator urokinase	NM_008873	-2.9	
Restin	NM_019765	-13.9	*Yellow
Ccl2	NM_011333	-154.6	*Crimson
TGF-a	NM_031199	-3.1	
TGFb-R3	NM_011578	-3.2	
Thrombospondin 1	NM_011580	-2.1	
Timp 1	NM_011593	-2.1	
TNF a	NM_013693	-26.8	*Black
Vcam 1	NM_011693	-2.9	
VEGF a	NM_009505	-7.8	*Orange
VEGF b	NM_011697	-9.5	*Navy Blue
Ribosomal Protein L13a	NM_009438	1.0	
PUC plasmid DNA	L08752	0.0	

Table 2. Densitometry of murine mammary tumor angiogenesis arrays. The color corresponds to the location of the gene in figure 2 (*). Genes that showed a two-fold or greater difference from control are presented. For normalization purposes, densitometry values that were measured as zero were assigned a normalized value of 10 to perform comparisons (**).

References

Albiston, A.L., et al. Evidence that the angiotensin IV (AT(4)) receptor is the enzyme insulin-regulated aminopeptidase. J. Biol. Chem. 276, 48623-48626, 2001.

American Cancer Society. Cancer Reference Information. April 13, 2003. http://www.cancer.gov

Alberghina L et al. Towards a blueprint of the cell cycle. *Oncogene* 20:1128-1134, 2001

Carmeliet P and Jain RK. Angiogenesis in cancer and other diseases. *Nature* 407:249-257, 2000

Christensen, JG et al. C-Met as a Target for human cancer characterization of inhibitors for therapeutic intervention. Cancer Letters 225:1-26, 2005.

Davis CJ, et al. AT(4) receptor activation increases intracellular calcium influs and induces a non-N-methyl-d-aspartate dependent form of long-term potentiation. Neuroscience 137:108-117, 2006.

Delehedde, M. et al. Proteoglycans: pericellular and cell surface multireceptors that integrate external stimuli in the mammary gland. *Journal of Mammary Gland Biology and Neoplasia*. 6:253-273, 2001

Evan GI and Vousden KH, Proliferation, cell cycle and apoptosis in cancer. *Nature* 411:342-348, 200

Ferrara N. Timeline: VEGF and the quest for tumor angiogenesis factors. *Nature Reviews Cancer*. 2:795-803, 2002

Fidler IJ. Timeline: The pathogenesis of cancer metastasis: the seed and soil hypothesis revisited. *Nature Reviews Cancer*. 3:453-458, 2003.

Folkman, J, E Merler, C Abernathy, and G Williams. Isolation of a tumor factor responsible for angiogenesis. *J Exp Med* 13(2): 275-288 (1971)

Hanesworth, J.M., Sardinia, M.F., Krebs, L.T., Hall, K.L., and Harding, J.W. Elucidation of a specific binding site for angiotensin II (3-8), angiotensin IV, in mammalian heart membranes. J. Pharmacol. Exp. Ther. 266, 1036-1042, 1993.

Harding JW, et al. Identification of an AII(3-8) [AIV] binding site in gunea pig hippocampus. Brain Res. 26:340-343, 1992.

Higuchi, O. and Nakamura, T. Identification and change in the receptor for hepatocyte growth factor in rat liver after parital hepatectomy of induced hepatitis. Biochem. Biophys. Res. Commun. 176, 599-607, 1991.

Hill, RP and Tannock IF. The Basic Science of Oncology. McGraw-Hill New York, 1998

Kramar EA, Wright JW, and Harding JW. Angiotensin II- and IV induced changes in cerebral blood flow. Roles of AT1, AT2, and AT4 receptor subtypes. Regul Pept. 68:131-138, 1997.

Lew. R.A., et al. Angiotensin AT4 ligands are potent, competitive inhibitors of insulin regulated aminopeptidase (IRAP). J Neurochem. 86, 344-350. 2003.

Michor F, Iwasa Y, and Nowak MA. Dynamics of cancer progression. *Nature Reviews Cancer*. 4:197-205, 2004

Paul, Stefan AM. et al. HIF at the crossroads between ishcemia and carcinogenesis. J*ournal of Cellular Physiology.* 200:30-40, 2004

Pennachetti, S, et al. Hypoxia promotes invasive growth by transcriptional activation of the met proto-oncogene. Cancer Cell. 3:347-61, 2003.

Ruhrberg, C. Growing and shaping the vascular tree: multiple roles for VEGF. *BioEssays* 25:1052-1060, 2003

Scarpino S. et al. Increased expression of Met protein is associated with up-regulation of hypoxia inducible factor-1 (HIF-1) in tumor cells in papillary carcinoma of the thyroid. *J Pathol*. 202:352-258, 2004.

U.S. Food and Drug Administration. Center for Drug Evaluation and Research. April 13, 2003. http://fda.gov

Wright JW and Harding JW. Important role for angiotensin III and IV in the brain renin-angiotensin system. 25:96-124, 1997.

Wright JW and Harding JW. The brain angiotensin system and extracellular matrix molecules in neural plasticity, learning, and memory. Prog Neruobiol. 72:263-293, 2004.

MANUSCRIPT I, NORLEUAL, AN AT_4 RECEPTOR LIGAND, IS A C-MET ANTAGONIST AND REPRESENTS A NEW CLASS OF ANTI-CANCER DRUGS

Introduction

Classic angiotensins are peptides that regulate cardiovascular function, water balance, and reproduction. These effects are predominantly mediated by the angiotensin one (AT_1) and angiotensin two (AT_2) receptors (1). More recently, a distinct angiotensin site was identified that selectively binds the hexapeptide angiotensin fragment, VYIHPF (Ang IV) (2) and has been characterized as the AT_4 receptor (3). Analogs of Ang IV induce a number of profound biological effects on central nervous system, renal, and cardiovascular function (4). The molecular identity of the target AT_4 receptor, however, has remained elusive. Here we report that an AT_4 ligand, Norleual, which shares homology with the hinge region of hepatocyte growth factor (HGF), competes with ^{125}I-HGF for high affinity binding to its receptor, Met. In addition, Norleual modulates HGF-dependent Met signaling and inhibits HGF-induced cell scattering. Furthermore, Norleual elicits anti-angiogenic effects in an aortic ring model and anti-cancer effects *in vivo* in a murine melanoma model that are consistent with Met antagonist behavior. These findings suggest that the mechanism of action of AT_4 ligands involves perturbation of the Met system and that AT_4 ligands may represent a novel drug family that would broaden treatment strategies for cancer and other diseases with Met dysfunction.

Text

Because Ang IV-like sequences are found in a variety of proteins besides angiotensinogen, a homologus-sequence-conservation screen was employed to identify potential endogenous ligands for the unidentified AT_4 receptor. One ligand that drew particular interest was hepatocyte growth factor (HGF) and by association its receptor, Met (**Fig. 3a**).

Met receptors are broadly distributed in human tissues and are most commonly expressed in cells of epithelial origin (5, 6). Coincidentally, putative AT_4 receptors have been found in an array of epithelial and nervous mammalian tissues that often differ in function and distribution from those enriched in AT_1 and AT_2 receptors (**Fig.3b**) (7). Moreover, the Met and AT_4 systems share a fundamental role in tissue remodeling. Both Nle^1-Angiotensin IV (Nle^1-Ang IV), an AT_4 receptor agonist (8) and HGF (9) have been shown to enhance neurite outgrowth and/or play an influential role in central nervous system development. Likewise, each system appears to exert a subset of its effects by regulating extracellular matrix-related molecules (4, 10). Because of the common actions of the Met and AT_4 systems, we hypothesized that these two systems could actually be one in the same.

To begin to probe for a potential interaction between AT_4 receptor ligands and Met, radioligand binding methods were employed to determine whether the AT_4 receptor antagonist, Norleual [Nle-Y-L-ψ-(CH_2-NH_2)-H-P-F] (11) could compete with HGF binding to Met. Both Norleual and HGF were observed to compete with ^{125}I-HGF for high affinity binding (**Fig. 3c**,**d**). The IC_{50} for Norleual

and HGF were 3.1 +/- 2.1 pM and 29.4 +/- 14.7 pM (mean +/- SEM, n=3) respectively; the later value was similar to that reported previously (12). To further test the hypothesis that Norleual interacts with the Met system, ^{125}I-Norleual was cross-linked to HEK293 cell membranes alone or in the presence of either HGF or Norleual. Both ligands competed for ^{125}I-Norleual-specific binding to HEK293 cell membranes (**Fig. 3e**,**f**). Together, these findings suggest that the AT_4 ligand Norleual interacts directly with Met.

We next asked whether the interaction of Norleual with Met had functional consequences on Met signaling. Like all type I receptor tyrosine kinase receptors, activation of Met can induce tyrosine residue phosphorylation and association of various signaling proteins (13,5). Critical to Met signaling is the association of growth factor receptor bound protein 2, Grb2 associated binder (Gab1), a multi-functional scaffolding adapter (5,6). Gab1 association provides c-Met with multiple docking sites for a variety of intracellular signal transducers (14). Accordingly, we asked whether Norleual could modulate either of these two features of Met activation. To address this question, HEK293 cells were activated by HGF in the presence or absence of Norleual. Solubilized membranes were immunoprecipitated (IP) with a Met antibody and immunoblotted (IB) for total Met (which allowed normalization of IB data) and IB for phospho-tyrosine, to detect the activated form of Met. **Fig. 4a** demonstrates that Met phosphorylation can be induced in a dose-dependent manner with saturation occurring at 550 pM HGF. Norleual alone did not alter Met phosphorlylation when compared to untreated samples (**Fig. 4b**). Yet, Norleual

at 20 and 50 pM significantly reduced HGF-dependent Met and Gab1 phosphorylation compared to HGF alone (**Fig. 4b,e**). In addition, Norleual significantly reduced HGF-initiated association between Gab1 and Met (**Fig. 4c,e**). To confirm these findings, treated HEK293 lysates were immunoprecipitated with Gab1 and IB for total Gab1 and phospho Gab1, its activated form. (**Fig. 4d**). Again, Norleual inhibited HGF-induced Gab1 phosphorylation. Collectively, these data indicate that the AT_4 antagonist Norleual markedly attenuates HGF-dependent Met activation (see also **Fig. 7**).

Met activation generally manifests cellular responses of increased proliferation/survival, motility, and differentiation (15). Together, these cellular changes contribute to Met's hallmark effects of scattering (16), a process characterized by decreased cell adhesion and increased motility, and branching morphogenesis (17). In order to explore the physiological significance of Norleual's ability to depress Met signaling, its effect on Met-dependent changes in cell scattering were examined. HGF's ability to induce cell scattering of Met expressing Madin-Darby canine kidney (MDCK) cells was assessed with the coverslip assay (**Fig. 5a,b**) (16). As expected, Norleual inhibited HGF-induced MDCK cell scattering (**Fig 5c**) yielding a response that was not different from untreated controls (**Fig. 5d**). Together these data demonstrate that Norleual not only competes with high affinity for HGF binding to Met, but is also a potent inhibitor of Met-dependent signaling and cell function. These findings suggest that Norleual may be effective at inhibiting Met-dependent actions *in vivo*.

The Met receptor is enriched on vascular endothelial cells where it plays a crucial role in the regulation of angiogenesis (18). NK4, a large molecule Met inhibitor, has been shown previously to inhibit angiogenesis (19). Since Norleual appears to act as a small molecule Met inhibitor, we predicted that Norleual would exhibit similar activity. To test this prediction, angiogenesis was evaluated with the *ex vivo* mouse aortic ring assay in the presence and absence of Norleual. After four days in culture, robust angiogenic sprouts were observed in control rings (**Fig. 6a**). Angiogenic growth was significantly attenuated in Norleual treated wells (**Fig. 6b**). Because Met activation in endothelial cells is a critical enabler of angiogenesis (20), we further predicted that Norleual should inhibit Met signaling in endothelial cells. In support of this idea, Norleual was observed to inhibit HGF-induced Met/Gab1 association in human umbilical vein endothelial cells (HUVEC) *in vitro* (**Fig. 6c**). Together, these observations indicate that inhibition of angiogenesis by Norleual may be attributed to the attenuation c-Met signaling in endothelial cells. However, interaction with other cell types and the microenvironment involved with the angiogenic process has yet to be explored.

The growing interest in c-Met as an anti-cancer target (21) and the recent use of anti-angiogenic molecules (22) such as Bevacizumab, an anti-VEGF antibody, for cancer therapy (23) led us to examine the effect of Norleual on *in vivo* tumor growth. As expected, Norleual inhibited primary B16 murine melanoma growth in male C57 mice (**Fig. 6d**). Because c-Met dysregulation in human melanoma results in enhanced proliferation and migration (24, 25) we

investigated the possibility that Norleual could inhibit HGF/c-Met signaling in melanoma cells, thus contributing to its anti-tumor activity. As anticipated, Norleual was observed to attenuate HGF-induced Met/Gab1 association in B16 murine melanoma cells cultured *in vitro* (**Fig. 6e**). This finding suggests that the basis for Norleual's efficacy corresponds to its behavior as a c-Met antagonist, by imparting a dual inhibition on angiogenesis and tumorigenesis (21).

Earlier studies had suggested that the biological activity of AT_4 ligands might be attributable to inhibition of the protease, the insulin regulated aminopeptidase (IRAP) and the resultant accumulation of bioactive peptides (26). Many of the observed biological characteristics of the AT_4 system, however, were difficult to reconcile with this IRAP model alone. This suggested that another identified protein(s) was responsible for the action of AT_4 receptor ligands (3,4). The findings presented here suggest that Met represents one such unidentified target and that the mechanism of action of Norleual is at least partly dependent on its ability to inhibit Met function. These studies indicate that Norleual competitively competes for HGF binding to Met, antagonizes HGF-dependent Met signaling activity *in vitro*, inhibits HGF-induced cell scattering *in vitro*, inhibits angiogenesis modeled *ex vivo*, and attenuates melanoma tumor growth *in vivo*. In addition, the apparent behavior of Norleual predictably matches that of a hypothetical Met antagonist by imparting a dual inhibition of Met activity in endothelial and Met expressing cancer cells.

The Met system is known to be dysregulated in many diseases as in human cancers (27) where it is involved in multiple steps of tumorigenesis,

metastasis, and tumor-associated angiogenesis (5,6,10). Consequently, development of Met antagonists as anti-cancer agents has been a priority for some time (6,20,24). Unfortunately, a detailed crystallographical understanding of the precise interaction between HGF and Met has yet to be attained, and consequently, the rational design of Met inhibitors has been hindered (21). AT_4 ligands may represent a new family of tools to uncover the intricacies of the HGF/Met system.

In addition to developing more efficacious anti-cancer drugs, pecuniary matters must also be considered. Therefore, scientific research that yields the development of inexpensive, easy to manufacture, small molecule inhibitors for cancer would be most beneficial (6,21,28). The AT_4 antagonist, Norleual, may represent a family of molecules that is both therapeutic and economical for cancer therapy. In conclusion, these findings provide new insight into the workings of the AT_4 receptor and identify a new family of Met antagonists that may allow novel cancer treatment strategies, improve accessibility, and lower the cost of therapy.

Material and Methods

Compounds

Norleual was synthesized by Syngene (Bangalore, India). Hepatocyte growth factor (HGF) was purchased from R&D systems (294-HGN).

Antibodies

Antibodies against c-Met, DO-24, 07-283, and DQ-13, were purchased from Upstate. Anti-phospho-tyrosine, HAM1676, was purchased from R&D systems and 06-427 was purchased from Upstate. Anti-Gab1, 06-579, was purchased from Upstate.

Cell Culture

Human embryonic kidney cells 293 (HEK293), Madin Darby canine kidney cells (MDCK), and B16BL6 were grown in DMEM, 10% fetal bovine serum (FBS). Human Umbilical Vein Endothelial Cells (HUVEC) were grown in EGM-2 (Cambrex). Cells were grown to 100% confluentcy before use. HEK and MDCK cells were serum starved for two hours and B16BL6 were serum starved for 48 hours before conducting treatments.

Iodination of ^{125}I-HGF and ^{125}I-Norleual

Carrier free HGF was iodinated using the chloramine T method described by Higuchi (12). 10μl of 1.5M $NaPO_4$ (pH 7.4), 4 μl ~ 1 mCi $Na^{125}I$ (Perkin Elmer), 10 μl of 1ng/ml HGF were placed in a 500 μl microcentrifuge tube. The reaction was started by adding 5 μl of 0.1 mg/ml chloramine-T which was added a total of four times at 90 second intervals. The reaction was halted by the addition of 50 μl of 50mM N-acetyl-l-tyrosine, 200 μl of 60 mM NaI, and 200 μl of 1.2 mg/ml

urea. ^{125}I-HGF was separated from free iodine by using a G-25 Sephadex (1.5 x 20 cm) gel filtration column and 20 mM sodium phosphate, 75 mM NaCl, and 0.1% BSA as the solvent with a flow rate of 0.5 ml/min. Fractions between 18 and 36 minutes were collected. Norleual was iodinated using the chloramine-T method described by Zhang (29). The reaction was performed in 0.2 M sodium phosphate buffer (pH 7.2) containing a total volume of 118 μl (50μl [1 ng/ml] Norleual, 50 μl additional buffer, 10μl chloramine T (4mg/ml), and 8μl consisting of 2 mCi Na^{125}I (Perkin Elmer). The reaction was incubated for 2 minutes at room temperature. The reaction was stopped by the addition of 50 μl $Na_2S_2O_5$ (5mg/ml). ^{125}I-Norleual was separated from free ^{125}I and di-iodinated Norleual by using a reverse phase C_{18} column (5 mm x 250 mm, Microsorb-MV, Rainin Instrument). Solvent A was 80 mM triethylamine phosphate (pH 3) and acetonitrile was used as solvent B. ^{125}I-Norleual was purified using a linear gradient of 9% – 25% B over 90 minutes.

^{125}I-HGF Binding Assay

Mouse liver was homogenized in hypotonic buffer fortified with 0.1% bovine serum albumin as described by Hanesworth (28). 600μg of membrane protein was incubated with 50pM ^{125}I-HGF with various concentrations of HGF or Norleual in a total volume of 100μl phospho-buffered-saline (PBS) fortified with 0.1% BSA. Binding was carried out for one hour on ice. Membranes were pelleted by centrifugation and unbound label was removed by washing the pellet twice with incubation buffer. Pellets were resuspended and radioactivity was counted with a gamma counter (Isomedic 10/880, ICN, Cost Mesa, CA).

^{125}I-Norleual Cross-linking Assay

HEK293 cells were grown to confluentcy in DMEM fortified with 10% FBS. Media was aspirated and cells were washed twice with ice-cold PBS. Cells were lysed with hypotonic buffer (1ml per 100mm plate) and homogenized as described by Hanesworth (30). 450μg of membrane protein was incubated with 1nM ^{125}I-Norleual with or without 15μM Norleual or 10nM HGF in a total volume of 300μl PBS. Binding was carried out for 50 minutes at room temperature (RT). Cross-liking was carried out for 30 minutes at RT with a final concentration of 2.5 mM bis-sulfosuccinimidyl suberate. The reaction was stopped by incubating for 15 minutes RT with Tris at a final concentration of 18mM. Membranes were pelleted by centrifugation, 20,000g, 4°C. The supernatant was removed and the pellet was washed three times with 750μl ice cold PBS. The pellet was dissolved in 100μl radioimmunoprecipitation base (RIPA, Upstate) for 15 minutes on ice. Pellets were spun at 14,000g, 4°C to pellet the insoluble materials. 90μl of supernatant was transferred to a fresh microcentrifuge tube containing 450μl PBS and loaded into a BioGel P6 column. The bound label was separated from free by centrifugation at 232g for 10 min as described by Zhang (29). The membrane cross-linked ^{125}I-Norleual was counted on a gamma counter.

Immunoprecipitation, Western Blotting

Cells were washed twice with PBS and serum starved for two hours in DMEM before HGF/compound treatment. Cells were harvested using RIPA base fortified with phosphatase inhibitor cocktails 1 and 2 (Sigma). Protein concentration was determined using the BCA total protein assay (Pierce).

Lysates were incubated with antibody overnight at 4°C with gentle agitation. Immunoprecipitation controls received mouse non-specific Ig (Upstate). Proteins were captured with protein-A agarose (Upstate) and were washed three times with phosphate-buffered-saline. Proteins were resolved using SDS-PAGE electrophoresis (Criterion, BioRad), and transferred to a nitrocellulose membrane. Membranes were incubated with appropriate primary antibodies and washed in water and PBS, 0.05% tween-20. Membranes were then incubated with appropriate secondary antibody (Pierce) and washed following Upstate protocols. Proteins were visualised using the Supersignal West Pico Chemiluminescent Substrate system (Pierce). Molecular weights were determined by comparison to protein ladders (BenchMark, Invitrogen and Kaleidoscope, BioRad). The film images were digitized and analyzed using Totallab® software.

Aortic ring assay

48-well plates (Falcon) were coated with Growth Factor Reduced Matrigel according to the manufacturer's protocol (BD Biosciences, thick gel method). Under microscopic dissection, the thoracic aorta of a 6 week-old C57 mouse was removed and cut into 0.5mm sections under aseptic conditions, washed in PBS, and placed in the Matrigel-coated wells. 100 μl of Matrigel was added and allowed to solidify for 30 min at 37°C to embed the rings. The rings are incubated for 24 hours in growth-factor-containing EGM-2 (Cambrex) at 37°C in 5% CO_2 /air. The medium is then replaced with basal medium, EBM (Cambrex) supplemented with 2% FBS and 10mg/ml gentamicin with or without Norleual at

10^{-10} M. Aortic rings were then incubated for four days at 37°C in 5% CO_2. Digital images were taken and angiogenic sprout area was measured using ImageJ (National Institutes of Health). Areas were normalized to aortic diameters.

Scattering assay

Using aseptic technique, coverslips were placed in six well plates. MDCK cells were grown to 100% confluency and washed twice with PBS. The coverslips were transferred to new six well plates containing 900 µl serum free DMEM. Norleual and HGF were added to appropriate wells. Control wells received PBS vehicle. Plates were incubated at 37°C with 5% CO_2 for 48 hours. Media was removed and cells were fixed with methanol. Cells were stained with Diff-Quik Wright-Giemsa (Dade-Behring). Digital images were taken. Coverslips were removed with forceps and more digital images were captured. Pixel quantification of images was done using ImageJ and statistics were performed by Prism.

In vivo melanoma cancer model

Six-month old male C57BL/6 mice were anesthetized with an intra peritoneal injection of ketamine/xylazine (10mg/kg in 0.01ml/g volume and 0.2mg/kg in 0.003ml/g volume respectively). Once under anesthetic, 500,000 B16BL/6 were dorsally injected intra-dermally. At the same time, a slow release ethylene vinyl acetate Elvax drug pellet (DuPont) containing Norleual were surgically implanted intramuscularly into the right gluteus maximus. Control animals were implanted with Elvax pellets containing an equal quantity of bovine serum albumin. The

dose of drug was calculated to be 21 μg/kg/day. Primary tumors were palpable within 10 days and termination of the experiment occurred on day sixteen. Palpated tumors were measured with digital calipers every two to three days. Tumor volumes were calculated using the equation: [$V = (4/3)*pi*r^3$]. Every day, each mouse was assessed visually for any signs of complications. Upon assessment, appropriate measures were taken if warranted (adhering to the guidelines of Part 3 of the Washington State University Guide for the Care and Use of Laboratory Animals). The predetermined endpoint of the experiment was a combination of two factors, tumor size ~3000 mm^3 and mouse morbidity. Mice were euthanized upon reaching either of these two endpoints.

Statistics

Independent one-way ANOVAs (InStat v.3.05) were used to determine differences among groups. Tukey-Kramar or Bonferroni's multiple comparison post-hoc tests were performed where necessary. Statistical comparisons of two groups were determined using the two-tailed Student's *t*-test (InStat and Prism) with a level of significance of 0.05.

FIGURE 3

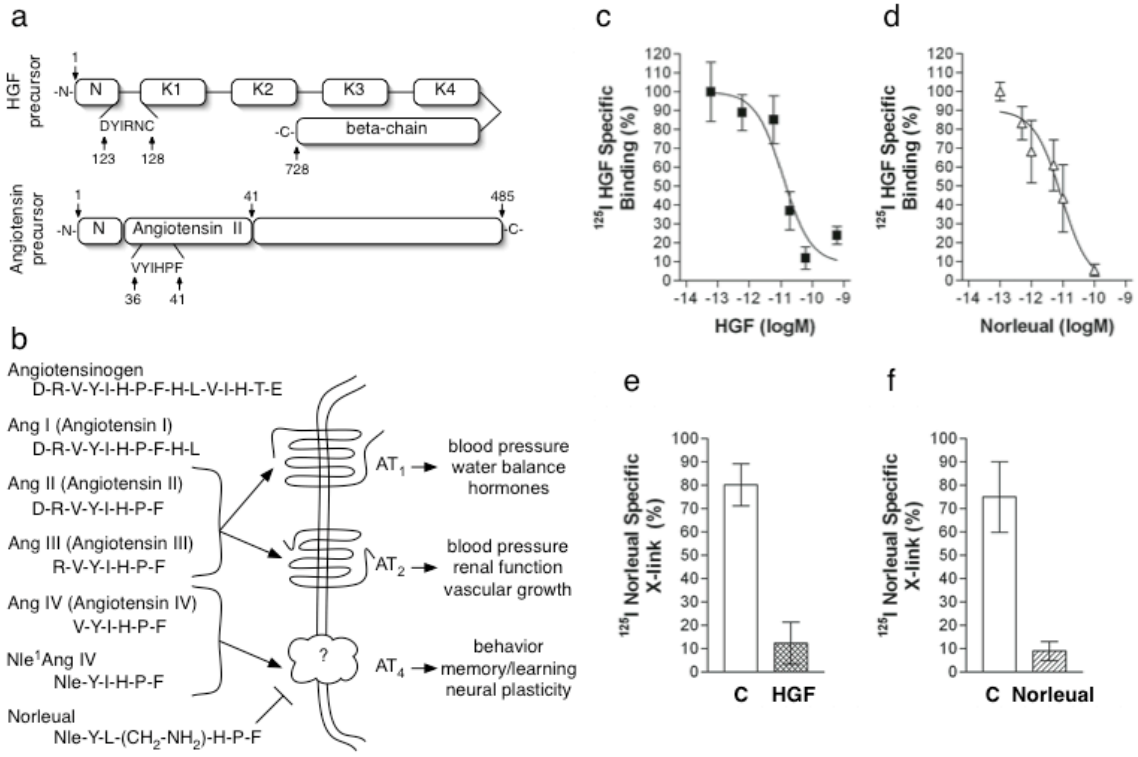

Figure 3. Norleual and HGF each compete for high affinity binding with ^{125}I-Norleual and ^{125}I-HGF (a) Homologous sequence comparison of HGF and angiotensin precursors. (b) A cartoon displaying the differential binding sites for the various angiotensin fragments and Norleual. (c and d) Mouse liver plasma membranes were incubated with 50 pM ^{125}I-HGF and indicated concentrations of HGF (■) or Norleual (△). Results are presented as percent of specific ^{125}I-HGF binding and error bars indicate +/- SEM. Competition experiments each included quadruplicate data points and each experiment was repeated in triplicate with an average HGF IC_{50} of 29 pM with a standard deviation of 29.4 and Norleual IC_{50} of 3.1 pM with a standard deviation of 4.1. (e and f) ^{125}I-Norleual was crosslinked to HEK membranes in the presence or

absence of HGF () or Norleual (). Specific binding is reported as percent control (). Error bars indicate +/- SEM, n=4.

FIGURE 4

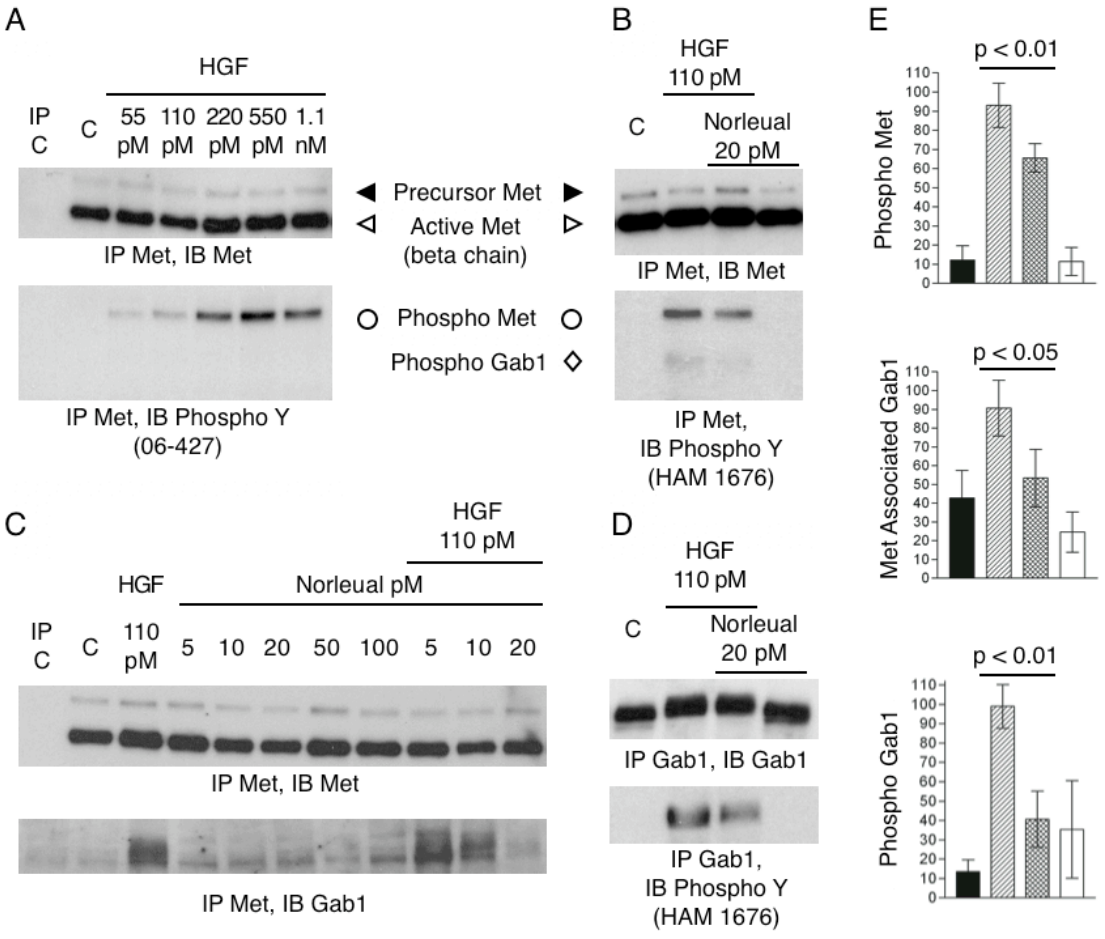

Figure 4. Norleual inhibits HGF dependent Met phosphorylation and Gab1 association and phosphorylation in vitro. (a) HEK293 cells were treated for 10 minutes with HGF at indicated concentrations. Lysates were immunoprecipitated (IP) with anti-Met (DO-24) and immunoblotted (IB) with anti-Met or anti-phospho tyrosine (06-427) (b) HEK293 cells were treated for 10 minutes with HGF and/or Norleual at indicated concentrations. Lysates were IP with anti-Met (DO-24) and IB with anti-Met (DQ-13) or anti-phospho tyrosine (HAM 1676, lot JLB03). (c) HEK293 lysates were IP with anti-Met (DO-24) and

IB with anti-Gab1. (d) HEK 293 lysates were IP with anti-Gab1 and IB with anti-Gab1 or anti-phospho tyrosine (HAM 1676). (e) Relative amounts (normalized to % total Met in IP) of quantified IP/IB band intensities for control (), 110 pM HGF (), 110 pM HGF and 20 pM Norleual (), and 20 pM Norleual () treated HEK293 cells for phospho-Met (n=4), phospho-Gab1 (n=4), and Met associated Gab1 (n=3). Error bars indicate +/- one standard deviation, and p values were determined by one-way ANOVA followed by Tukey-Kramer multiple comparison test.

FIGURE 5

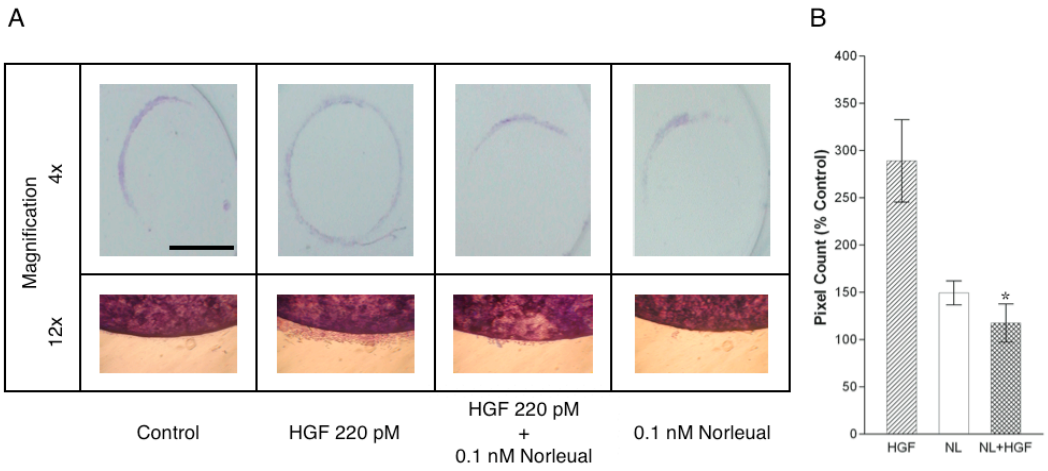

Figure 5. Norleual inhibits HGF induced cell scattering in MDCK cells. (a) MDCK cells were grown to confluency on coverslips and were transferred to six-well plates before treatment with vehicle (n=4), HGF (▨, n=6), HGF + Norleual (▩, n=6), or Norelual (□, n=4), for 48 hours. Cells were fixed and stained with crystal violet. (Top) 12x magnification of MDCK scattering off of coverslips (Bottom) 4x magnification after coverslips had been removed. Scale bar, 6mm. (b) Pixel quantification analysis of cell scattering off of coverslips. Values were normalized to average control values. Normalized values were compared using ANOVA. The difference between HGF vs. HGF + Norleual groups was significant as determined by Bonferroni's multiple comparison test, ($p<0.01$).

FIGURE 6

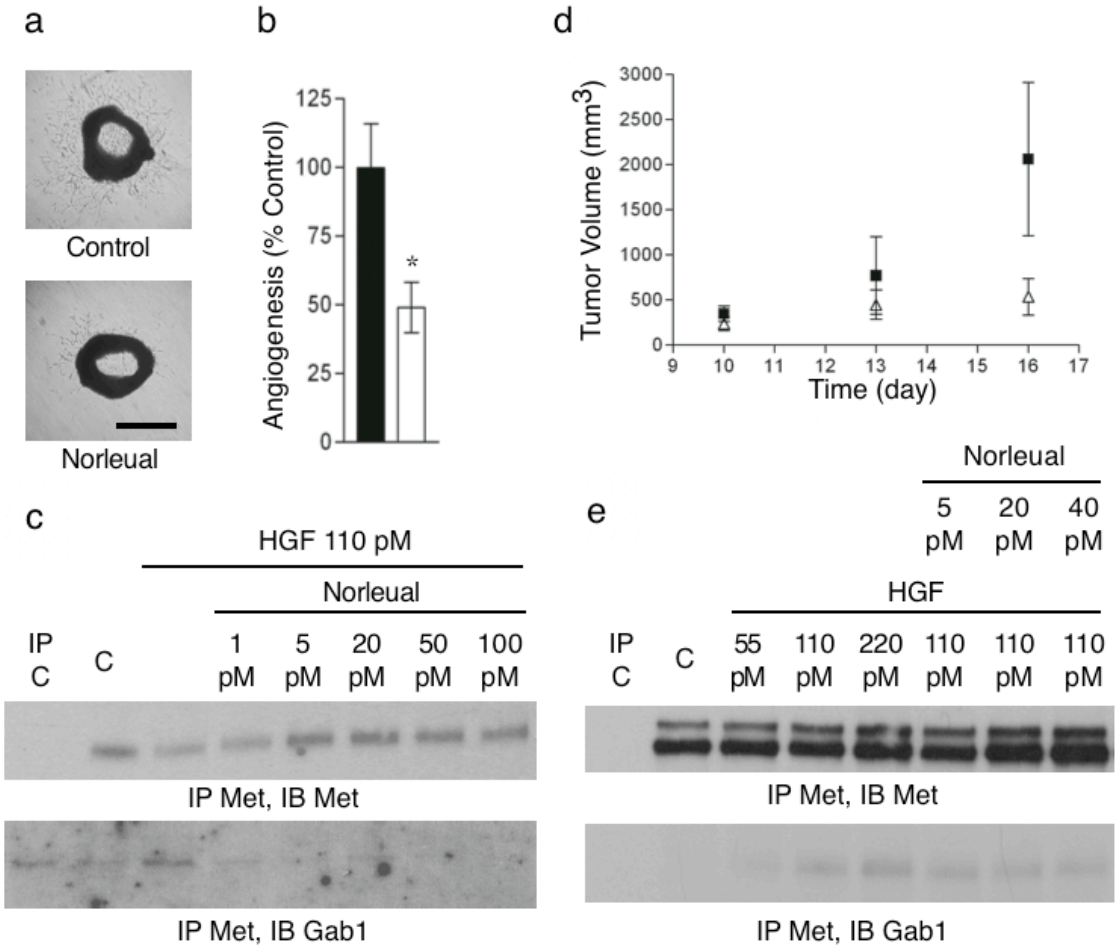

Figure 6. Norleual inhibits angiogenesis and melanoma growth. (a) Norleual inhibits angiogenesis in the mouse aortic ring assay. Mouse aortas were cut into 0.5 mm sections and imbedded in Matirgel. Rings were incubated in EGM-2 media (Cambrex) with (n=8) or without (n=6) Norleual for four days. Digital photos of the rings were taken on day four. Scale bar is approximately 2 mm. (b) Quantification of aortic ring angiogenesis. Areas covered by angiogenic sprouts were quantified from day four ring photos control (▬) and Norelual (▭) treated. A p-value of 0.012* was obtained from a two tailed p-test and error bars indicate +/- SEM. (c) HUVECs were treated for 5 minutes with HGF

and/or Norleual at indicated concentrations. Lysates were IP with anti-Met and IB with anti-Met, anti-phospho tyrosine, or Gab1. (d) C57BL/6 mice were inoculated with B16 murine melanoma cells. Control (■) or Norleual (△) slow release Elvax pellets were implanted inter-muscularly . Tumor size was asssessed with digital calipers and tumor volumes were calculated (n=6), error bars indicate +/- standard deviation. (e) B16 cells were treated for 8 minutes with HGF and/or Norleual at indicated concentrations. Lysates were immunoprecipitated (IP) with anti-Met and immunoblotted (IB) with anti-Met or Gab1.

FIGURE 7

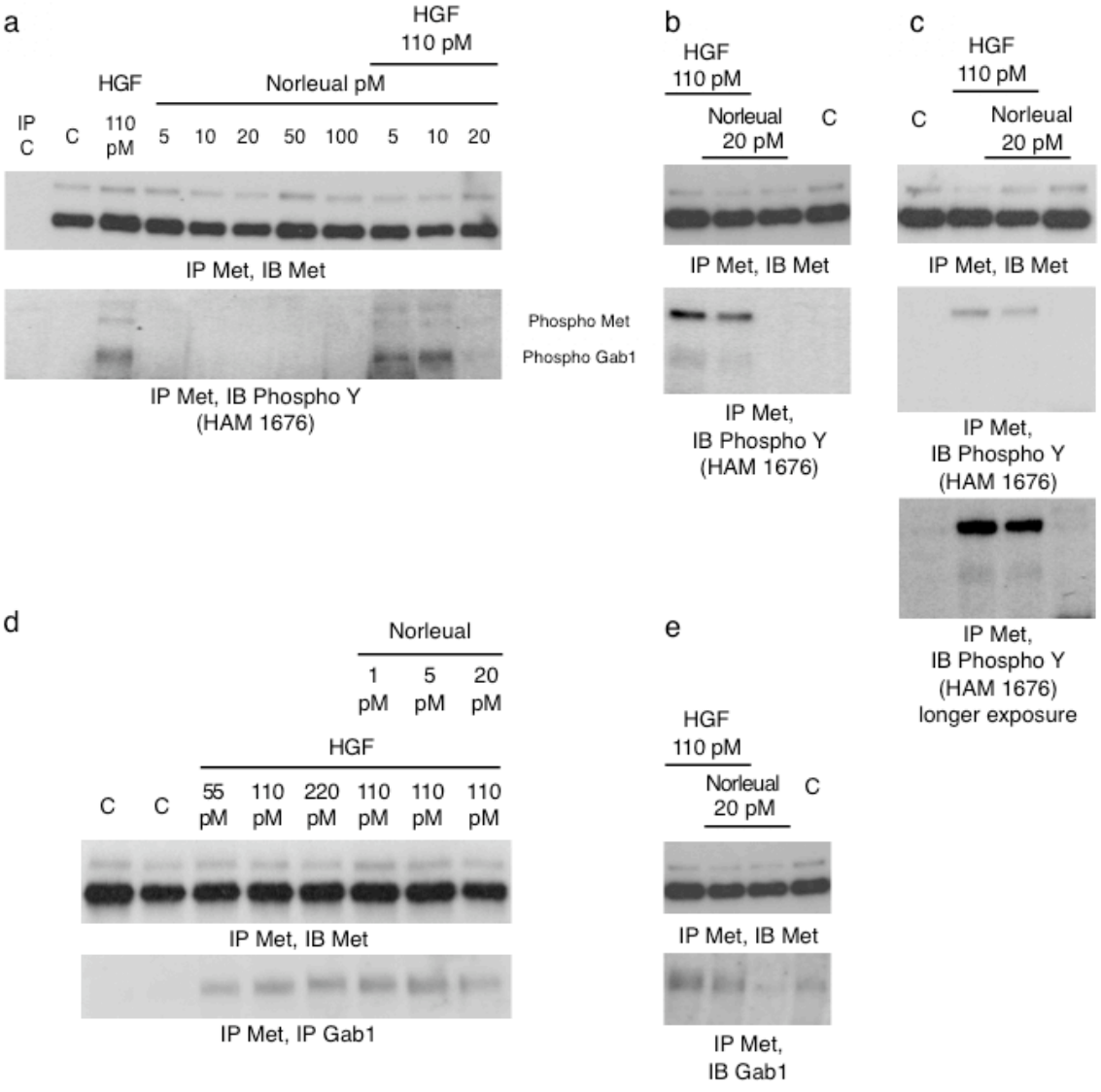

Figure 7. Norleual inhibits HGF dependent Met phosphorylation and Gab1 association and phosphorylation *in vitro*. (a,b, and c) HEK293 cells were treated for 10 minutes with HGF at indicated concentrations in the presence or absence of Norleual. Lysates were immunoprecipitated (IP) with anti-Met and immunoblotted (IB) with anti-Met or anti-phospho tyrosine (a, HAM1676 lot JLB02), (b and c, HAM1676 lot JLB03). (d and e) HEK 293 cells were treated for 10 minutes with HGF and/or Norleual at indicated concentrations. Lysates were

IP with anti-Met (DO-24) and IB with anti-Met (DQ-13) and IB with anti-Gab1 (06-579).

Acknowledgments

We thank Christina Russert, Humam Kadara, and Bryan Hudson for technical assistance, Suzanne Lindsey for HGF, and Gary Meadows and Ya-Min Fu for the B16BL6 cells. Lastly, we would like to thank Michael Varnum for contributions and critical review of this paper. These studies were funded by a grant from Pacific Northwest Biotechnology, Inc. (PNB), Pullman, WA. Both J. W. Harding and J. W. Wright are shareholders in PNB.

References

1. McKinley, M.J., et al. The brain renin-angiotensin system: location and physiological roles. *Int. J. Biochem. Cell Biol*. **35**, 901-918 (2003).
2. Harding, J.W., et al. Identification of an AII(3-8) [AIV] binding site in guinea pig hippocampus. *Brain Res.* **26**, 340-343 (1992).
3. Harding J.W., Wright J.W., Swanson, G.N., Hanesworth, J.M., and Krebs, L.T., AT4 receptors: specificity and distribution. *Kidney Int.* **46**, 1510-1512 (1994).
4. Wright, J.W., and Harding, J.W. The brain angiotensin system and extracellular matrix molecules in neural plasticity, learning, and memory. *Prog. Neruobiol.* **72**, 263-293, (2004).
5. Birchmeier, C.,Birchmeier, W., Gherardi, E., and Vande Woude G.F. Met, metastasis, motility and more. *Nat. Rev. Mol. Cell Biol.* **4**, 915-925 (2003).
6. Corso, S., Comoglio, P.M., and Giordano S. Cancer therapy: can the challenge be MET? *Trends Mol. Med.* **11**, 284-292. (2005).
7. Wright J.W. and Harding J.W. Brain angiotensin receptor subtypes AT1, AT2, and AT4 and their functions. *Reg. Peptides.* **59**, 269-295 (1995).
8. Wright J.W. and Harding J.W. Important role for angiotensin III and IV in the brain-renin-angiotensin system. *Brain Res. Rev.* **25**, 96-124. (1997).
9. Maina, F., et al. Multiple roles for hepatocyte growth factor in sympathetic neuron development. *Neuron* **20**, 835-846 (1998).
10. Gentile, A. and Comoglio, P.M. Invasive growth, a genetic program. *Int. J. Dev. Biol.* **48**, 451-456. (2004).
11. Davis, C.J., et al. AT4 receptor activation increases intracellular calcium influx and induces a non-N-methyl-D-aspartate dependent form of long term potentiation. *Neuroscience.* **137**, 1369-1379 (2005).
12. Higuchi, O. and Nakamura, T. Identification and change in the receptor for hepatocyte growth factor in rat liver after parital hepatectomy of

induced hepatitis. *Biochem. Biophys. Res. Commun.* **176**, 599-607 (1991).
13. Naldini, L. et al. The tyrosine kinase encoded by the MET proto-oncogene is activated by autophosphorylation. *Mol. Cell Biol.* **1250**, 1085-1100. (1991).
14. Trusolino L., and Comoglio, P.M. Scatter-factor and semaphoring receptors: cell signaling for invasive growth. *Nat. Rev. Cancer.* **2**, 289-300. (2002).
15. Zhang, Y.W. and Vande Woude, G.F. HGF/SF-met signaling in the control of branching morphogenesis and invasion. *J. Cell Biochem.* **88**, 408-417. (2003).
16. Miao, H., et al. EphA kinase activation regulates HGF-induces epithelial brahching morphogenesis. *J. Cell Biol.* **162**, 1281-1292 (2005).
17. Berdichevsky F., Alford, D., D'Souza, B., and Taylor-Papadimitriou, J. Branching morphogenesis of human mammary epithelial cells in collagen gels. *J. Cell Sci.* **107**, 3557-3568. (1994).
18. Rosen, E.M. and Goldberg, I.D. Regulation of angiogenesis by scatter factor. *EXS*. **79**, 193-208 (1997).
19. Kuba, K. et al. HGF/NK4, a four-kringle antagonist of the hepatocyte growth factor, is an angiotenesis inhibitor that suppresses tumor growth and metastasis in mice. *Cancer Res*. **60**, 6737-6743. (2000).
20. Jiang, W.G., et al. Hepatocyte growth factor, its receptor, and their potential value in cancer therapies. *Crit. Rev. Oncol. Hematol.* **53**, 35-69 (2005).
21. Zhang, Y.W., Graveel, C., Shinomiya, N., and Vande Woude G.F. Met decoys: will cancer take the bait? *Cancer Cell* **6**, 5-6 (2004).
22. Folkman, J., Heymach J., and Kalluri R. *Tumor angiogenesis. In cancer medicine, 6th edition.* (editor Kufe, D.W. et. al.) p. 157-191. B.C. Decker, Hamilton, Ontario, Canada.
23. Folkman. J. Angiogenesis. *Annu. Rev. Med.* **57**, 1-18. (2006).
24. Christensen, J.G., Burrows, J., and Salgia, R. c-Met as a target for human cancer and characterization of inhibitors for therapeutic intervention. *Cancer Lett.* **225**, 1-26 (2005).
25. Recio, J.A., and Merlino G. Hepatocyte growth factor/scatter factor activates proliferation in melanoma cells through p38 MAPK, ATF-2, and cyclin D1. *Oncogene* **21**, 1000-1008 (2002).
26. Albiston, A.L., et al. Evidence that the angiotensin IV (AT(4)) receptor is the enzyme insulin-regulated aminopeptidase. *J. Biol. Chem.* **276**, 48623-48626 (2001).
27. Danilkovitch-Miagkova, A. and Zbar B. Dysregulation of Met receptor tyrosine kinase activity in invasive tumors. *J. Clin. Invest.* **109**, 863-867. (2002).
28. Shrag D. The price tag on progress. *N. Engl. J. Med.* **351**, 317-319. (2004).

29. Zhang, J.H., et al. Structural analysis of angiotensin IV receptor (AT_4) from selected bovine tissues. *J. Pharmacol Exp. Ther.* **289**, 1075-1083 (1999).
30. Hanesworth, J.M., Sardinia, M.F., Krebs, L.T., Hall, K.L., and Harding, J.W. Elucidation of a specific binding site for angiotensin II (3-8), angiotensin IV, in mammalian heart membranes. *J. Pharmacol. Exp. Ther.* **266**, 1036-1042 (1993).

MANUSCRIPT 2, NORLEUAL INHIBITS MURINE MELANOMA IN VIVO

Abstract

The *in vivo* anti-cancer effects of Norleual, the AT_4 and Met antagonist, have been previously limited to murine breast cancer models and a single murine melanoma experiment. Due to the potential clinical value of Norleual as a Melanoma therapy, we further developed this initial finding using more sophisticated methods. We observed that the anti-melanoma activity of Norleual is maintained in female mice. Furthermore, we observe that drug efficacy is retained when administered *in situ* after tumors are established. Moreover, we observe a non-classical dose response of Norleual that is common among angiogenesis inhibitors. Together, these findings encourage the potential of Norleual as a clinical and perhaps broad range cancer therapeutic.

Introduction

In 2005, it was estimated that over 59,000 Americans would be diagnosed with melanoma skin cancer. Sadly, over 7,000 will die from this disease (American Cancer Society, 2005). Despite advances in scientific research, patients diagnosed with stage IV melanoma only have a 10% five-year survival rate (American Cancer Society, 2005). For this reason, new and effective melanoma and other cancer treatments must be developed. Despite this urgency, many of the new and successful cancer drugs (except for angiogenesis inhibitors) are often only therapeutic for a distinct niche in a single cancer type, let alone efficacious for a broad range of cancers. Therefore, it would be beneficial to develop a cancer drug that could be used as a broad-spectrum

cancer therapeutic. Interestingly, one target is commonly deregulated among cancers of epithelial origin. This target is c-Met (Jiang, 2005, Christensen, 2005).

Since the discovery of the hepatocyte growth factor (HGF)/c-Met receptor tyrosine kinase system over twenty years ago, HGF/Met activity has been shown to induce mitogenic, motogenic, and morphogenic cell responses (Zhang and Vande Woude 2003). Understandably, Met activity has been linked to invasive growth and branching morphogenesis which today have become the classical c-Met responses. Today, we know that Met is implicated in the physiologies and pathologies of angiogenesis, axon guidance, cancer, and others (Birchmeier 2003). Because Met signaling appears to be a major gateway to invasive growth, branching morphogenesis, and cell survival, functional integrity of the Met system is absolutely critical. Consequently, corruptions of the Met system contribute to the pathogenesis of many diseases (Trusolino and Comoglio, 2002). Furthermore, it is believed that Met signal transduction plays a role in malignant and invasive development of neoplasms (Corso 2005). Predictably, HGF/c-Met malfunctions have been identified in a number of cancers. Met expression is detected in approximately 79% and overexpressed in 21% of human breast cancers surveyed (22/28, 6/28 respectively) (Christensen, 2005). Interestingly, in melanoma tumors also surveyed by SUGEN, 71% of the tumors expressed and 36% overexpressed c-Met (10/14, 5/14 respectively). Recently, it was suggested that the AT_4 antagonist and Met antagonist, Norleual, inhibits male murine melanoma growth *in vitro* (Yamamoto, unpublished). However, this finding remains unsubstantiated, and further development and exploration in

melanoma application must be conducted. In this paper, we expand preliminary findings that Norleual inhibits murine melanoma.

Materials and Methods

Cell culture

B16BL/6 cells were cultured in DMEM supplemented with 100U/ml penicillin, 100μg/ml streptomycin and 10% fetal bovine serum (FBS). For injection, cell cultures were grown in 100mm plates to 90% confluentcy. The media was aspirated and replaced with 3ml 0.25% trypsin/EDTA solution (Sigma) warmed to 37°C. Cell detachment was monitored using an inverted microscope. Upon detachment, 10ml serum free DMEM was added, and the entire contents were transferred to a 15 ml conical vial. Suspensions were then centrifuged for 10-15 min at 600 rpm to pellet the cells. The supernate was aspirated and the pellet was resuspended with 600μl hank's balanced salt solution (HBSS). All cell suspensions were then combined and well mixed. Aliquots of 200μl were transferred to 500μl microcentrifuge tubes and kept on ice. 100μl of this cell suspension was ultimately injected, resulting in a homograft of approximately 500,000 cells.

In vivo model

Six-month old male C57BL/6 mice were anesthetized with an intra peritoneal injection of ketamine/xylazine (10mg/kg in 0.01ml/g volume and 0.2mg/kg in 0.003ml/g volume respectively). Once under anesthetic, 500,000 B16BL/6 were dorsally injected intra-dermally. Primary tumors were palpable within 10 days and termination in approximately 20 days. Palpated tumors were

measured with digital calipers every two to three days. Tumor volumes were calculated using the equation for volume of an ellipsoid: [$V = (4\pi/3)*(l/2)^2*(w/2)$].

Elvax pellet drug delivery

Norleual containing Elvax pellets were prepared per manufacturer's protocol (DuPont). Elvax pellet release was calculated by determined release rate to be 1/400 of total content per day.

Injection drug delivery

After grafting, mice were randomly assigned into appropriate groups. Mice received a daily administration of drug or vehicle comprising of a 25ul saline or drug/saline injection via 0.33cc insulin syringe (29g needle) intramuscularly or *in situ*. A schedule of four injection sites were rotated through the right and left gluteus medius and right and left biceps femoris to allow for recovery of the injection site. Every day, each mouse was assessed visually for any signs of complications (excessive inflammation/infection). Upon assessment, appropriate measures were taken if warranted (adhering to the guidelines of Part 3 of the Washington State University Guide for the Care and Use of Laboratory Animals). The predetermined endpoint of the experiment was a combination of two factors, tumor size ~3000 mm^3 and mouse morbidity. Mice were euthanized upon reaching either of these two endpoints.

Statistical analysis

Tumors were measured using digital calipers. Tumor volumes were estimated based upon two-dimension tumor measurements. From these

measurements, tumor growth curves were created in Prism and differences in growth were tested for significance using InStat (ANOVA).

Results

Previously, it was demonstrated that Noreual inhibits murine melanoma in vivo in male mice (Yamamoto, unpublished). Because this study was conducted in male mice, we wanted to determine if Norleual efficacy differed among sex. Accordingly, we conducted a study of Norleual murine melanoma efficacy in C57BL/6 female mice. Norleual was delivered via Elvax pellets implanted in the hind leg (27 μg/kg/day). We observed that Norleual retained efficacy in the female murine melanoma in vivo model (figure 8). This finding suggests that Norleual efficacy in murine B16 melanoma is not dependent upon sex.

Next, we wanted to investigate Norleual's efficacy on established melanoma tumors. B16 tumors were developed in C57BL/6 males to approximately 400 mm^3 in volume after thirteen days incubation *in vivo*. On day thirteen, Norleual was injected *in situ* at two doses (300 and 30 μg/kg/day). This treatment was continued for 48 more hours. We observed that a single administration, Norleual was able to hinder tumor growth rate (figure 9). Furthermore, this inhibition was stabilized until the third day where half of the Norleual treated tumors had grown substantially while the other half remained relatively the same size. This finding suggests that the tumors were eventually able to develop some resistance to Norleual. This finding is not surprising for drug resistance is a common phenomenon for all cancer therapies. It is assumed that the tumors are ultimately able to select for mutations that

eventually override the anti-angiogenic shift induced by the angiogenesis inhibitor (Carmeliet, 2005). In an effort to locate Norleual's therapeutic threshold, we conducted another experiment were we allowed the tumors to grow to a volume of 800 mm^3 before administering Norleual. We found that Norleual had no effect on the growth rate of these tumors (data not shown). This finding suggests that a neoplastic burden threshold exists between 400 and 800 mm^3 to where Norleual is no longer effective.

To investigate the dose response of Norleual, we conducted a study were Norleual was administered in various doses in the murine melanoma model used previously. In addition, to improve the accuracy and consistency of the administered dose, we modified the drug delivery method to IM injections. B16 melanoma tumors were grafted and mice received Norleual treatments every 24, 48, or 72 hours. These dosing intervals translated to doses of 21, 10, and 7 μg/kg/day, respectively. The 24 and 48-hour Norleual treated mice exhibited similar growth curves to those observed in the previous IM Elvax pellet experiments. However, the anti-tumor effect observed in the lowest dose, 7 μg/kg/day, was most dramatic (figure 10). During the experiment, the control animals, 24-hour, and two of the 48 hour Norleual treated mice were euthanized on day 20. Surprisingly, the survival period of the 72-hour Norleual treated mice was about 50% greater than the control mice. The mice on the 72-hour Norleual dose survived until day 28 when one mouse was removed from the study. On day 29, the rest of the Norleual 72-hour group was sacrificed and the experiment

was terminated. These findings suggest that the lower Norleual dose of 7 μg/kg/day is the most therapeutic out of the three doses administered.

Discussion

Because targeting Met would likely elicit a dual effect on cancer by antagonizing the Met systems on both the cancer cells and endothelial cells, we decided to investigate if Norleual efficacy in a murine melanoma model. We administered Norleual in different variations of drug delivery methods and experimental designs of the B16 murine melanoma C57BL/6 homograft *in vivo* model. Our findings suggest that the anti-tumor effects of Norleual are not dependent upon sex (figures 8, 9, and 10). Additionally, when Norleual is delivered in situ, the anti-tumor effect can be observed in a single treatment on developed tumors approximately 400 mm^3 (figure 9). However, the anti-tumor effect was no longer effective when the tumors were grown to 800 mm^3 before Norleual administration. Additionally, we observed a reverse-dose response of Norleual on B16 melanoma tumors *in vivo*. Unexpectedly, the lowest dose generated the greatest anti-tumor effect (figure 10). Encouragingly, non-classical dose response characteristics are common among anti-angiogenic compounds such as endostatin (Folkman, 2006). It is plausible that this notion is applicable to Norleual as well. If this is true, then in order to obtain the greatest therapeutic amplitude, Norleual must be titrated to a yet-to-be determined optimal dose. Furthermore, it is problematical to directly compare Norleual's efficacy based upon the different delivery methods, for the precise drug distribution parameters are unknown. At this point in time, such undertaking is arduous because no

method to quantify Norleual serum levels, nor levels at the active site (tumor) exist. Our future goal is to develop such assay systems so that these studies become feasible. Once some of Norleual's pharmacokinetic parameters are established, we can begin to arbitrate reliable conclusions relevant to the reverse-dose response phenomena. These future studies will also generate valuable data and methods that will facilitate clinical trial design and practicality.

FIGURE 8

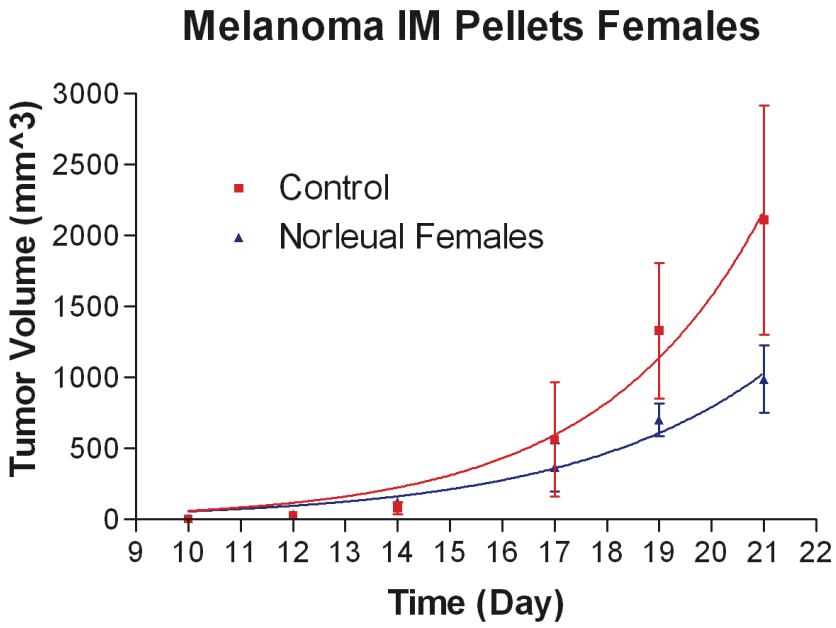

Figure 8. Pilot Study: *In vivo* inhibition of murine melanoma cancer growth by Norleual via systemic delivery 5 X 10^5 B16 murine melanoma cancer cells were subcutaneous injected along the dorsal midline of female C57BL/6 mice (n=2). An Elvax slow-release pellet (0.3 mg pellet) containing an inactive angiokine (control) or Norleual was simultaneously inserted intramuscularly (IM) into the gluteus maximus. The dose given was calculated to be approximately 37 μg/kg/day. Tumors were measured at various time points and tumor volume was calculated.

FIGURE 9

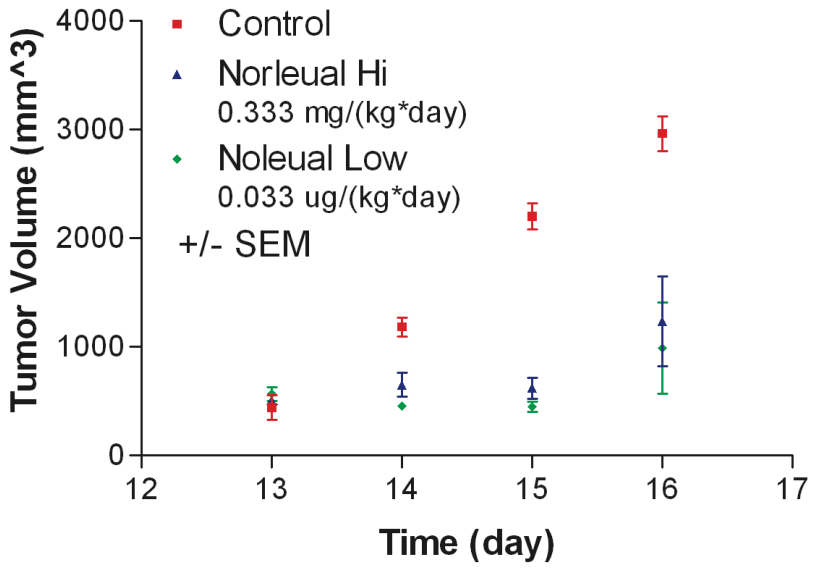

Figure 9. *In Vivo* inhibition of murine melanoma cancer growth by Norleual via in situ delivery. 5 X 10^5 B16 murine melanoma cancer cells were subcutaneous injected along the dorsal midline of male C57BL/6 mice (control n=5, Norleual n=4). Norleual or vehicle was injected *in situ* on days 13, 14, and 15 at indicated doses. Tumors were measured with digital calipers at various time points and tumor volume was calculated.

FIGURE 10

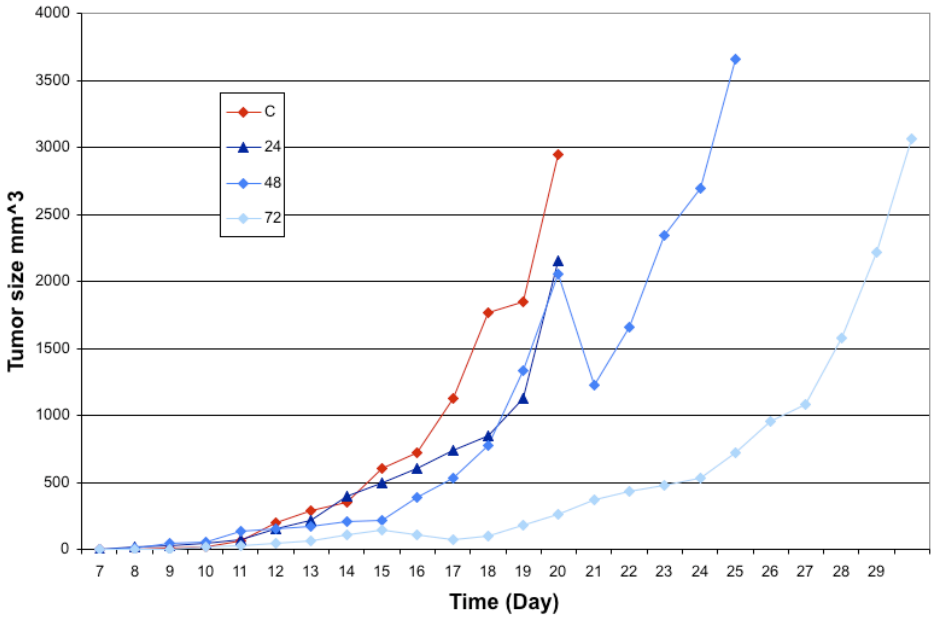

Figure 10. Norleual exhibits non-classical dose response in murine melanoma cancer via systemic delivery. 5 X 10^5 B16 murine melanoma cancer cells were subcutaneous injected bilaterally staggered across the dorsal midline of male C57BL/6 mice (n=8). Norleual or vehicle was injected inter muscularly at indicated times beginning on day two. (Control (red) received vehicle, 24 (dark blue): 0.21 μg/kg/day, 48 (blue): 0.105 μg/kg/day, 72 (light blue): 0.07 μg/kg/day) Tumors were measured with digital calipers at various time points and tumor volume was calculated. Error bars were not included because mice were intermittently removed from the study due to signs of morbidity (most evident in 48 hour Norleual treatment on day 20-21). At day 28, 100% of the original 72-hour Norleual group was included in the measurements. On day 29, 75% of the original 72-hour Norleual group was included.

References

American Cancer Society. Cancer Reference Information. Feb 6, 2006. http://www.cancer.org

Birchmeier, C et al. Met, metastasis, motility and more. Nat Rev Mol Cell Biol 4, 915-25, 2003.

Carmeliet P. Angiogenesis in life, disease and medicine. Nature. 438:932-936, 2005.

Christensen, JG et al. C-Met as a Target for human cancer characterization of inhibitors for therapeutic intervention. Cancer Letters 225:1-26, 2005.

Corso, S, Comoglio PM, and Giordano S. Cancer therapy: can the challenge be MET? *Trends in Mol Med.* 11:284-292, 2005.

Folkman, J. Angiogenesis. Annu. Rev. Med. 57:1-18, 2006.

Jiang WG. Et al. Hepatocyte growth factor, its receptor, and their potential value in cancer therapies. Crit Rev in Oncol/Hematol. 53:35-69, 2005.

Trusolino L. and Comoglio PM. Scatter-factor and semaphoring receptors: cell signaling for invasive growth. Nature. 2:289-299, 2002.

Zhang YW and Vande Woude GF. HGF/SF-Met signaling in the control of branching morphogenesis and invasion. J Cell Biochem. 88, 408-17, 2003.

MANUSCRIPT 3, TOXICOLOGICAL STUDY OF NORLEUAL IN A C-57BL/6 MURINE MODEL

Abstract

The AT_4 antagonist Norleual has been shown to elicit anti-cancer efficacy in vitro and in vivo. Furthermore, it has been suggested that the mechanism of action of Norleual involves the HGF/Met system. Because Norleual has potential usefulness as a clinical cancer therapeutic, potential side effects must be identified. Accordingly, we performed a toxicological study of Norleual in C-57BL/6 mice at one hundred times the therapeutic dose established in our murine melanoma studies, 21 μg/kg/day. Over the course of one hundred days, Norleual treated mice grew at a much slower rate than control animals. This finding was further investigated with dual energy x-ray (DEXA) analysis which revealed Norleual treated mice were significantly lower in percent body fat, but not lean body mass. Further blinded pathological assessment yielded no signs of additional major gross or microscopic toxicity other than fewer lipid vacuoles in zones II and III in Norleual treated animals. These findings indicate that a toxicity of the AT_4 antagonist and c-Met antagonist, Norleual, is reduction in body fat composition that may be related to liver vacuole deposition.

Introduction

Recently, the AT_4 antagonist, Norleual, was shown to have anti-cancer and anti-angiogenic effects. Moreover, it has been suggested that these effects involve attenuation of the hepatocyte growth factor/c-Met receptor tyrosine kinase system. Therefore, the potential for Norleual and perhaps other AT_4

ligands to be used as cancer therapies remains unlimited. One important question that remains unanswered is what are the potential side effects of Norleual? Previously, toxicological information about Norleual was second handedly obtained while conducting thirty week long chronic Norleual treatments on transgenic adenocarcinoma of mouse prostate (TRAMP) models. Although these studies suggested that Norleual was effective in inhibiting primary prostate tumor growth (data unpublished), unique observations regarding possible side effects of Norleual were also made during the course of this pilot study. Even though there were no observable differences in cage manners between treated and control animals, the treated animals presented a differing phenotype when compared to control animals. The treated animals appeared to be “thinner” and “narrower” in appearance. Unfortunately, due to the nature, design, and stage of these studies, it was impossible to obtain quantitative data on these observations.

Due to the fact that Norleual is intended for potential use as a clinical cancer therapy, it is imperative that it be determined whether or not these observations are scientifically significant and are indeed adverse side effects of Norleual. Therefore, we set out to conduct a study where we would investigate these and other potential side effects of chronic Norleual treatment in healthy, five week old, C57BL/6 male mice.

Materials and Methods

Mouse model

Twenty-four five-week old C57BL/6 male mice were equally and randomly assigned to two groups. One group was assigned as control and the other treated. Treated mice were administered intermuscular (IM) injections of Norleual at 21 μg/kg/day, (40 μl injectable volume) every 48 hours for the duration of one hundred and one days. Injection sites were rotated between left and right gluteus medius. BD Ultra-Fine 3/10 cc insulin syringes were used as delivery apparatus. Mice were housed two per cage and had unlimited access to food and water. Mice were monitored daily for signs of morbidity. Mice were also weighed on a weekly basis.

From the original study of twenty-four mice, two mice were removed from the study. One mouse originated from the control group. Mouse # C9 weighed 16g on day 0. However the average weight for control mice was 26g +/-1.8g (standard deviation). This mouse was an obvious runt of the litter and was a statistical outlier in weight. Hence this control mouse was removed from the study. Another mouse, from the Norleual treatment group, T7, was also removed from the study. On day 5, this mouse received a Norleual injection in the right gluteus medius. After injection the mouse appeared to be sluggish in appearance and within 10 minutes, had passed away. The mouse was dissected to determine if the injection had caused gross hemorrhage, leading to death. However, no signs of acute injury could be located. Because this was a singular incident out of 277 other injections, we believe that the cause of death is more likely to be due to the stress associated with IM injection rather than acute Norleual toxicity. For example, if cause of death were due to acute Norleual

toxicity, one would expect to observe instances of mortality. This phenomenon was not observed. Furthermore, no other mice displayed signs of declining health after any of the other injections. Except for this single incident, Norleual had no observable effect on the overall health and well being of the mice. However, despite this explanation, the death did occur to a member in the Norleual treated group, and certainty of cause of death cannot be definitively assigned at this point. Thus, the experimental data was analyzed with n=11 for each control and Norleual treated group.

Body composition analysis

To assess body composition, the Comparative Orthopedic Research Laboratory at the Washington State University Veterinary School was utilized. A Hologic QDR4500A fan beam dual-energy X-ray absorptiometer (DXA) was used to assess the lean body mass (muscle), fat, and bone composition of each mouse on day one hundred one of the experiment. Mice were sacrificed (explained in pathology) and DXA scans were performed. Due to the volume limitations of the DXA and pathology, half of the mice were sacrificed and analyzed on day 101. The remaining mice were sacrificed and analyzed 22 hours later. Control and treated mice were spit evenly among the two sacrifice episodes. Data was collected and the control group was compared to the Norleual treated group by two-tailed student's t-tests using InStat. Figures were created in Prism.

Pathology

Mice were sacrificed on day one hundred one by hypobaric CO_2 chamber. Specimens were shipped on ice to Dr. Patrick Caplazi at the Veterinary Pathology Dept of Veterinary Population Medicine and Veterinary Diagnostic Laboratory, College of Veterinary Medicine, University of Minnesota. Samples were harvested and analyzed in a blinded fashion. Mice were dissected and a gross dissection and assessment of organs was performed. Tissues were harvested, fixed, mounted, stained with hematoxylin and eosin, and evaluated by a pathologist. Data was then matched to control and treated mice and the results were qualitatively tabulated in the form of a table.

Results

Twenty-four, five-week old, C57BL/6 male mice were randomly spit into two groups, control and treated. Over the course of one hundred one days, each treated mouse received an intra muscular (IM) injection every forty-eight hours in the right or left glueteus medius. The dose, 21 μg/kg/day, was administered by IM injection at one hundred times the therapeutic dose determined in previous murine melanoma studies. Mice were monitored daily for signs of morbidity and were weighed weekly to assess weight gain.

Over the course of the study, apart from the exceptions explained below, no Norleual treated mice exhibited any signs of morbidity or observable deleterious health complications. This was also observed for the control mice. However, after a few weeks of treatment, it was apparent that the Norleual treated mice were different in appearance than the control mice. Akin to the long-term prostate cancer study, Norleual treated mice again displayed a

thinner/narrower and shorter phenotype when compared to control mice. This observation is evident in the growth curves for each group (figure 11 A). By the end of the study, the physical difference between the groups was most pronounced (figure 11 B). From these observations, we formed the question does the differential in weight due to differences in fat and/or lean body mass.

To quantify these observations, dual-energy X-ray absorption (DXA) analysis was performed (figure 12 A). The measured DXA masses of Norleual treated mice were significantly lower than control mice (figure 12 B right). This finding was confirmed when the actual mouse weights were compared (figure 12 B left). DXA scans also revealed that the Norleual treated mice were significantly smaller than control mice (figure 12C). In addition, the DXA analysis also measures body composition. Furthermore, there was no difference in bone mineral density (figure 12 D). Interestingly, the DXA analysis revealed that the Norleual treated mice had lower percentage of body fat when compared to control animals (figure 12 E). Interestingly, there was no difference in lean body mass (figure 12 F). This data suggests that the weight loss observed in the Norleual treated animals is due to differences in adipose tissue deposition and not lean body mass or bone mineral density.

Because of the significant discrepancy in percent body fat, we questioned whether Norleual was also affecting other tissues or organs. Accordingly, we performed a blinded pathological assessment of all twenty-two mice. In accordance, the pathology confirmed the differences in body mass measured previously (data not shown). Furthermore, the mass of the epidydimal fat bodies

matched the trend observed in the DXA analysis; the epidydimal fat bodies in the control animals appeared to be larger compared to the epidydimal fat bodies (Figure 13 A and B) in Norleual treated animals. These findings were confirmed when the weights of the epidydimal fat pads were compared (data not shown). In addition, microscopic pathology was also conducted on major organs (Figure 13 C). Surprisingly, there were no major differences in lesions in all the tissues surveyed. The only discrepancy was Norleual treated animals exhibited fewter number of lipid vacuoles in liver zones II and III. Because Norleual is a potent HGF/c-Met antagonist, there is good probability that Norleual could be affecting hepatocytes directly. However, because Norleual is also known to inhibit angiogenesis (Masino and Harding, unpublished), we decided to investigate blood vessel deposition in the epididymal fat bodies by factor eight staining. Unfortunately, the pathology report was inconclusive, and no reliable conclusion could be made.

Met is a receptor tyrosine kinase that stimulates a range of biological responses ranging from proliferation, motility, differentiation, and apoptotic protection. Together, these responses are elemental in Met's pivotal role in invasive growth that is fundamental to angiogenesis and branching morphogenesis (Gentile and Comoglio. 2004). Invasive growth is a tightly regulated and coordinated event that is most prominent in development (Larue and Bellacosa), but also plays a vital role in adults. Although typically quiescent, invasive growth is activated in responses of inflammation, wound repair, menstrual cycling, and angiogenesis (Comoglio, 2002). Today, we know that

dysregulated angiogenesis is implicated in over seventy diseases that includes cancer (Carmeliet 2005). In cancer, if the tumor cannot recruit additional blood supply, the net tumor growth remains constant (Folkman). Consequently, research of anti-angiogenic agents has been at the forefront of scientific research as cancer therapeutics.

The anti-tumor and anti-angiogenic, AT_4 antagonist, and c-Met antagonist, Norleual displays promising potential as a cancer therapeutic (Yamamoto, unpublished). However the potential side effects of Norleual have not been established. Here, we conducted a toxicological study of Norleual in healthy C57BL/6 mice to investigate potential side effects. We report that C57 mice chronically administered Norleual at 21 μg/kg/day sustained significant weight loss. Furthermore, the weight discrepancy was determined to be body fat and not lean body mass nor bone mineral content. This conclusion was similarly determined in a blinded pathology of the mice. Moreover, the results of the pathology study suggest that Norleual at 21 μg/kg/day is relatively non-toxic to mice. Furthermore, the only noticeable difference acquired from the pathology was that Norleual treated mice presented fewer lipid vacuoles in the liver than control mice. It is possible that Norleual is inhibiting the normal function of the adipocytes and negatively impacting adipose tissue deposition. However, future studies will have to be done in order to test this hypothesis.

In conclusion, these observations indicate that Norelual hinders murine weight gain and percent body fat. Based upon previous knowledge that Norleual is an HGF/c-Met antagonist and that we do observe physiological changes in the

liver, it is possible that Norelual could have an impact on normal liver function. However, at this juncture, the physiological relevance is unknown.

FIGURE 11

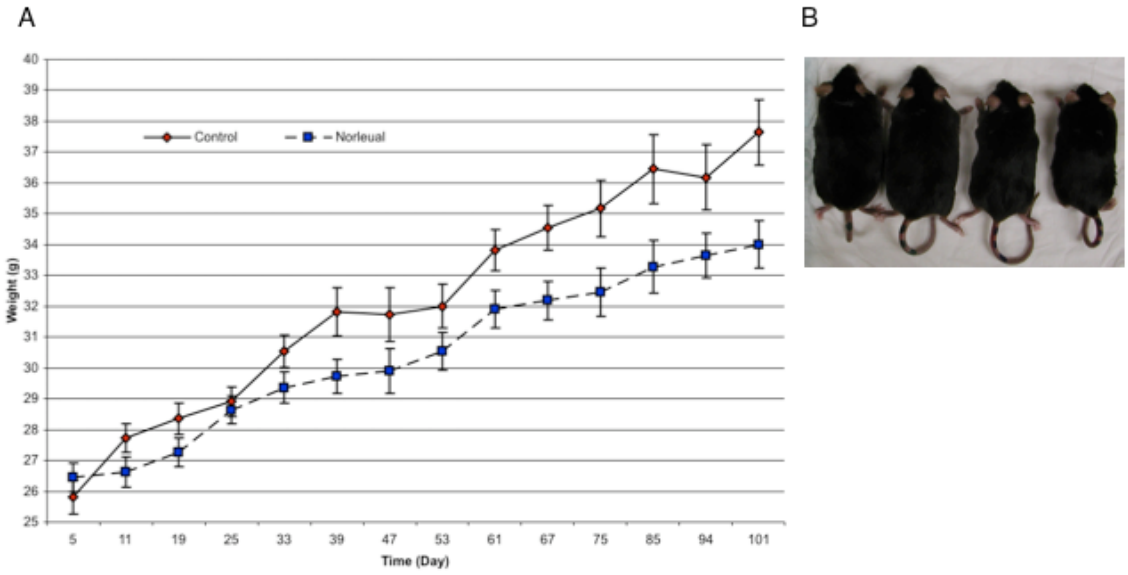

Figure 11. Growth profiles for control and Norleual treated mice. (A) C57 mice were treated with Norleual chronically for 101 days. Mice were weighed on a weekly basis. The average weights for each group, control (diamonds) and Norleual (squares) are shown over time. Error bars indicate +/-SEM and n=11. (B) Photo of mice at day 101. The two mice on the left are from the control group, while the two mice on the right are from the Norleual treatment group.

FIGURE 12

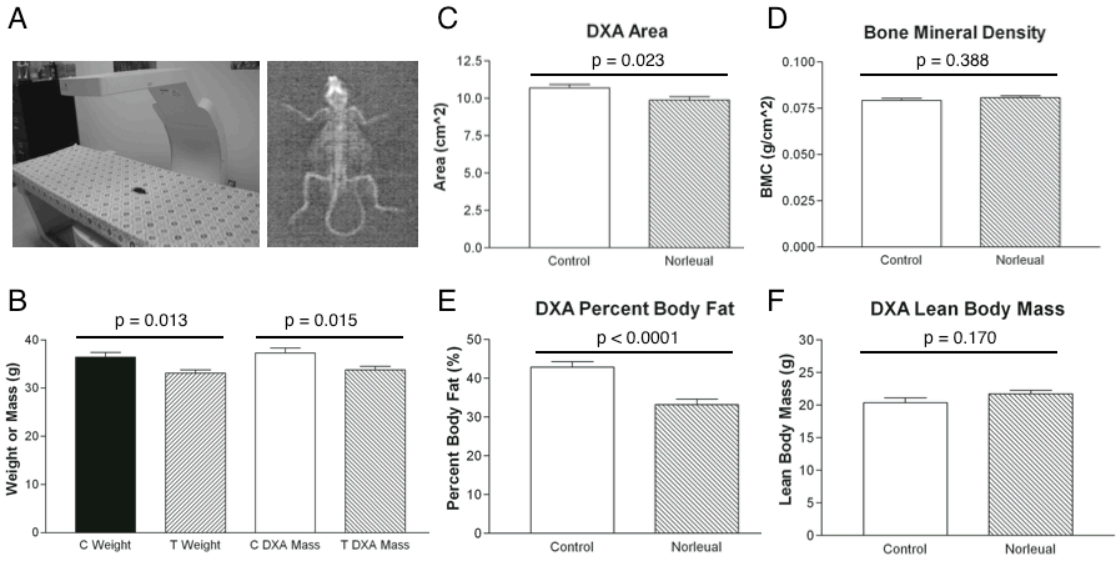

Figure 12. DXA analysis of Norleual treated and Control mice. (A) Left photo is a mouse on the DXA apparatus. The photo on the right is an x-ray image created by the DXA machine. (B) Comparison of mouse weights determined by scale measurement and DXA measurement on day 101. Left, scale measured weights of Norleual treated mice (hatched left) were significantly lower than control mice (black) (p=0.0130). Right, DXA measured mass of Norleual mice (hatched right) was significantly lower than control mice (white) (p=0.0146). (C) The DXA measured area of Norleual treated mice (hatched) was significantly lower than control mice (white) (p=0.023). (D) The DX measured bone mineral density was not statistically significant between Norleual treated mice (hatched) and control mice (white). (E) The percent fat of Norleual treated mice (hatched) was significantly lower than control mice (white) when measured by DXA (p<0.0001). (F) The lean body mass + bone mineral content (BMC) of Norleual treated mice

(hatched) was not significantly different than control mice (white) when measured by DXA ($p=0.18$). All error bars in figure 2 indicate SEM and $n=11$.

FIGURE 13

A

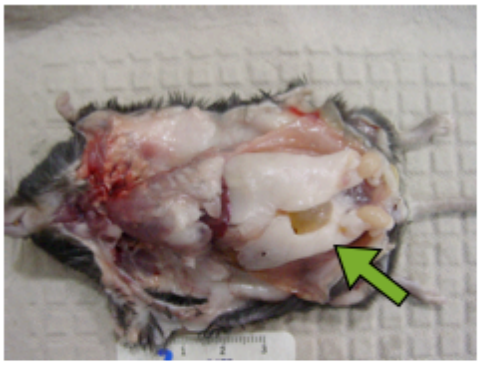

B

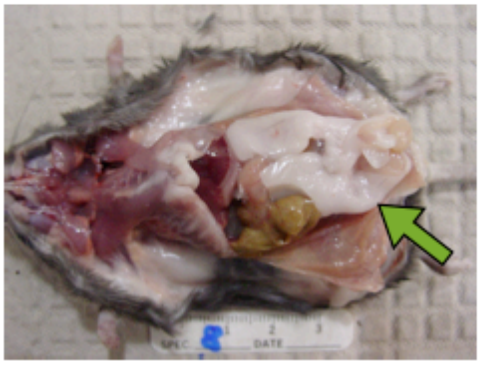

C

Organ	Location/Lesion/ Abnormality	Severity/Grade Control	Norleual
Brain	nsl	-	-
Heart	nsl	-	-
Spleen	nsl	-	-
Liver	Necrosis	++	++
	Lipid Vacuoles	+++	+
	Centrilobular Vacuolar Change	++	++
	Multifocal Random Necrosis	+	+
Pancreas	Islets/nsl	-	-
	Acini/nsl	-	-
Stomach	nsl	-	-
Small Intestine	Autolysis	+	+
Large Intestine	nsl	-	-
Kidneys	nsl	-	-
Prostate	nsl	-	-
Testes	nsl	-	-
Epididymis	nsl	-	-
Fat	Steatitis/Multifocal Random	+	+
Thyroid	nsl	-	-
Parathyroid	nsl	-	-
Adrenal Cortex	nsl	-	-
Adrenal Medula	nsl	-	-

Figure 13. Pathological assessment. Mice were subject to gross and microscopic pathological evaluation in blinded fashion. Dissections of a control mouse (A) and Norleual treated mouse (B) are shown. Green arrows point to the epidydimal fat pads. A summary of the pathology is shown in panel C (n=11).

Acknowledgments

We would like to thank Kelly Hughes for DXA scans.

References

Carmeliet P. Angiogenesis in life, disease and medicine. Nature. 438:932-936, 2005.

Comoglio PM and Trusolino L. Invasive growth: from development to metastasis. J. Clin. Invest. 109:857-862, 2002.

Crandall DL, et al. A review of the microcirculation of adipose tissue: anatomic, metabolic, and angiogenic perspectives. *Microcirculation.* 4:211-232, 1997.

Larue L. and Bellacosa A. Epithelial-mesenchymal transition in development and cancer:role of phosphatidylinositol 3' kinase/AKT pathways. Oncogenen. 24:7443-54, 2005.

Liu L and Meydani M. Angiogenesis inhibitors may regulate adiposity. *Nutr Rev*. 61:284-387, 2003.

Neels JG, Thinnes T, and Loskutoff DJ. Angiogenesis in an in vivo model of adipose tissue development. *FASEB J*. 18:983-985, 2004.

North MA. Advances in the molecular genetics of obesity. *Curr Opin Genet Dev*. 9:283-288, 1999.

Rehman J, et al. Obesity is associated with increased levels of circulating hepatocyte growth factor. *J Am Coll Cardiol.* 41:1408-1413, 2003.

Rupnick MA, et al. Adipose tissue mass can be regulated through the vasculature. *Proc Natl Acad Sci USA*. 99:10730-10735, 2002.

Shiota A, et al. A delted form of human hepatocyte growth factor stimulates hepatic lipogenesis and pipoprotein synthesis in rats. *Pharmacol Res.* 42:443-452, 2000.

Silha, JV, et al. Angiogenic factors are elevated in overweight and obese individuals. *Ins J Obes*. 29:1308-1314, 2005.

Swierczynski J, et al. Serum hepatocyte growth factor concentration in obese women decreases after vertical banded gastroplasty. *Obes Surg*. 15:803-808, 2005.

Trusolino L. and Comoglio PM. Scatter-factor and semaphoring receptors: cell signaling for invasive growth. Nature. 2:289-300, 2002.

Voros G, et al. Modulation of angiogenesis during adipose tissue development in murine models of obesity. *Endocrinology*. 146:4545-4554, 2005.

CONCLUSION

In this dissertation, we present evidence that an AT_4 antagonist, Norleual, interacts with the c-Met system and modulates c-Met function *in vitro, ex vivo*, and *in vitro*. In addition, we observe that Norleual behavior matches that of a hypothetical c-Met antagonist. This discovery suggests that other AT_4 ligands may also interact with this receptor system. Because c-Met function is critical for many important physiologies and is dysregulated in diseases other than cancer, AT_4 agonists and antagonists may be useful tools in counteracting c-Met dysfunction in disease.

Furthermore, the potential power of these compounds is demonstrated by the observed biological potency. We also show that Norleual exhibits potent anticancer effects in murine melanoma models with μg/kg/day quantities. Also preliminary toxicological findings indicate that Norleual is relatively non-toxic to mice. Together these findings illustrate that the future use of AT_4 ligands as clinical tools to inexpensively treat cancer and other diseases remain optimistic. In conclusion this dissertation brings AT_4 to a vantage from where we can see a new horizon of challenges and questions ahead. Do other AT_4 ligands interact with the Met system? Do AT_4 ligands interact with other proteins/receptors? Do we observe any selectivity? Does the anticancer effect of Norleual translate to humans? Are AT_4 ligands therapeutic for other diseases besides cancer? In the future, with ingenuity, dedication, hard work, and fortuity we will fashion answers to these questions and continue to expand our scientific knowledge and develop new medicines to placate our fellow mankind.